



**HAL**  
open science

## Multi-Knock-a multi-targeted genome-scale CRISPR toolbox to overcome functional redundancy in plants

Yangjie Hu, Priyanka Patra, Odelia Pisanty, Anat Shafir, Zeinu Mussa Belew, Jenia Binenbaum, Shir Ben Yaakov, Bihai Shi, Laurence Charrier, Gal Hyams, et al.

### ► To cite this version:

Yangjie Hu, Priyanka Patra, Odelia Pisanty, Anat Shafir, Zeinu Mussa Belew, et al.. Multi-Knock-a multi-targeted genome-scale CRISPR toolbox to overcome functional redundancy in plants. *Nature Plants*, In press, 10.1038/s41477-023-01374-4 . hal-04059773

**HAL Id: hal-04059773**

**<https://cnrs.hal.science/hal-04059773v1>**

Submitted on 5 Apr 2023

**HAL** is a multi-disciplinary open access archive for the deposit and dissemination of scientific research documents, whether they are published or not. The documents may come from teaching and research institutions in France or abroad, or from public or private research centers.

L'archive ouverte pluridisciplinaire **HAL**, est destinée au dépôt et à la diffusion de documents scientifiques de niveau recherche, publiés ou non, émanant des établissements d'enseignement et de recherche français ou étrangers, des laboratoires publics ou privés.

1       **Multi-Knock – a multi-targeted genome-scale CRISPR toolbox to overcome functional**  
2       **redundancy in plants**

3       Yangjie Hu<sup>1</sup>, Priyanka Patra<sup>1,2,\*</sup>, Odelia Pisanty<sup>1,\*</sup>, Anat Shafir<sup>1</sup>, Zeinu Mussa Belew<sup>3</sup>, Jenia Binenbaum<sup>1</sup>, Shir Ben  
4       Yaakov<sup>1</sup>, Bihai Shi<sup>2</sup>, Laurence Charrier<sup>4</sup>, Gal Hyams<sup>1</sup>, Yuqin Zhang<sup>1</sup>, Maor Trabolsky<sup>1</sup>, Omer Calderaru<sup>1</sup>, Daniela  
5       Weiss<sup>1</sup>, Christoph Crocoll<sup>3</sup>, Adi Avni<sup>1</sup>, Teva Vernoux<sup>2</sup>, Markus Geisler<sup>4</sup>, Hussam Hassan Nour-Eldin<sup>3</sup>, Itay  
6       Mayrose<sup>1,✉</sup>, and Eilon Shani<sup>1,✉</sup>

7  
8       <sup>1</sup> School of Plant Sciences and Food Security, Tel Aviv University, Tel Aviv, 69978, Israel

9       <sup>2</sup> Laboratoire Reproduction et Développement des Plantes, Université de Lyon, ENS de Lyon, CNRS, INRAE,  
10       Lyon, France

11       <sup>3</sup> DynaMo Center, Department of Plant and Environmental Sciences, University of Copenhagen, Frederiksberg,  
12       1871, Denmark

13       <sup>4</sup> Department of Biology, University of Fribourg, CH-1700 Fribourg, Switzerland

14       \* Equal contribution

15       ✉ Corresponding author

16  
17       **Abstract**

18       Plant genomes are characterized by large and complex gene families that often result in similar and partially  
19       overlapping functions<sup>1</sup>. This genetic redundancy severely hampers current efforts to uncover novel  
20       phenotypes, delaying basic genetic research and breeding programs<sup>2</sup>. Here, we describe the development  
21       and validation of Multi-Knock, a genome-scale CRISPR toolbox that overcomes functional redundancy in  
22       *Arabidopsis* by simultaneously targeting multiple gene-family members, thus identifying genetically  
23       hidden components. We computationally designed 59,129 optimal single guide RNAs (sgRNAs) that each target  
24       2 to 10 genes within a family at once. Furthermore, partitioning the library into ten sub-libraries directed towards  
25       a different functional group allows flexible and targeted genetic screens. From the 5,635 sgRNAs targeting  
26       the plant transcriptome, we generated over 3,500 independent *Arabidopsis* lines that allowed us to identify  
27       and characterize the first known cytokinin tonoplast-localized transporters in plants. With the ability to  
28       overcome functional redundancy in plants at the genome-scale level, the developed strategy can be readily  
29       deployed by scientists and breeders for basic research and to expedite breeding efforts.

### 33 **Introduction**

34 Plant genomics research and breeding programs rely on variation, be it natural, induced, or introduced.  
35 Phenotypic variation has been the basis for the identification of novel traits and their introduction into robust  
36 elite cultivars. Genetic variation has been expanded over the years by introducing natural variation and by  
37 creating random mutagenized lines by treatment with physical (e.g., radiation), chemical (e.g., ethyl  
38 methanesulfonate), or biological (e.g., T-DNA insertion or gene silencing) mutagens<sup>3-9</sup>. These approaches  
39 have greatly facilitated and accelerated progress in plant functional genomics and breeding programs over  
40 the past several decades.

41 Comprehensive genetic studies and large-scale genome sequencing projects have shown that it is  
42 challenging to uncover many phenotypes due to widespread genetic redundancy in plant genomes. A  
43 recurrent history of whole-genome duplications and numerous local duplications of smaller scale over the  
44 course of plant evolution has resulted in large gene families of similar sequences and partially overlapping  
45 functions. On average, 64.5% of plant genes are part of paralogous gene families, ranging from 45.5% in  
46 the moss *Physcomitrella patens* to 84.4% in the apple *Malus domestica*<sup>1</sup>. Given that ancient and fast-  
47 evolving paralogs are not easily detected due to sequence divergence, these percentages are likely  
48 underestimates. In *Arabidopsis* (*Arabidopsis thaliana*), the paralogous gene content, genes belonging to  
49 families with at least two members, vary from 63% to 78% depending on the methodological procedures  
50 applied<sup>1,4</sup>. It is speculated that single-copy genes are involved in the maintenance of genome integrity and  
51 organelle function, whereas multi-copy genes encode proteins involved in signaling, transport, and  
52 metabolism<sup>10</sup>. Therefore, in many cases mutating multiple gene family members is required to uncover  
53 "hidden" phenotypes associated with gene functions<sup>2</sup>.

54 Approaches creating random mutations for forward-genetics (e.g., alkylating agents and T-DNA lines)  
55 cannot overcome the limitations of genetic redundancy by simultaneously targeting multiple homologous  
56 genes in a single mutant line<sup>5,11</sup>. In recent years, significant progress has been made using genome-scale  
57 RNA interference methods and artificial microRNA (amiRNA) collections<sup>4,8,9</sup>. However, these methods do  
58 not work well in several important crops and generally reduce gene expression rather than cause complete  
59 knockout phenotypes<sup>12</sup>.

60 Recently, the CRISPR/Cas9 system (Clustered Regularly Interspaced Short Palindromic Repeats),  
61 involving CRISPR repeat-spacer arrays and Cas proteins, has been used to build large knockout mutant  
62 libraries for forward-genetic screens and analysis of gene functions and regulation. This system represents  
63 a tremendous breakthrough for generating targeted mutations both in terms of simplicity and efficiency<sup>13,14</sup>.  
64 In the past few years, studies have demonstrated the feasibility of CRISPR-based knockout collections in  
65 rice (*Oryza sativa* L.), maize (*Zea mays*) and tomato (*Solanum lycopersicum*)<sup>12,15-22</sup>. However, thus far,

66 CRISPR/Cas9 has not been used on a genome-scale level to simultaneously target multiple potentially  
67 redundant genes in plants or other eukaryotes.

68 Here, we describe the development and validation of Multi-Knock, a novel genetic approach in plants that  
69 combines forward-genetics with dynamically targeted genome-scale CRISPR/Cas9 tools to address the  
70 problem of masked phenotypic variation due to functional redundancy (**Fig. 1**). A total of 59,129 multi-  
71 targeted sgRNAs, divided into 10 functional sub-libraries targeting 16,152 genes in *Arabidopsis*, were  
72 designed, synthesized, and cloned into a genome-editing intronized Cas9 vector<sup>23</sup>. From this collection,  
73 5,635 sgRNAs targeting 1,123 of the 1,327 transporters (TRP) in *Arabidopsis* were cloned into four  
74 different Cas9 vectors generating independent CRISPR libraries, wherein each sgRNA was designed to  
75 target closely related homologues within sub-clades in transporter families. A proof of concept forward-  
76 genetic screen using over 3,500 CRISPR lines targeting the plant transportome recovered multiple known  
77 phenotypes in *Arabidopsis*, demonstrating the validity of the approach. Moreover, our screen allowed us to  
78 uncover novel transporters whose function has been hidden due to genetic redundancy. Specifically, we  
79 identified a homologous subfamily of three previously unstudied genes with partially overlapping function,  
80 *PUP7*, *PUP21*, and *PUP8*. We discovered that while all three proteins biochemically function as cytokinin  
81 transporters, *PUP8* localizes to the plasma membrane, while *PUP7* and *PUP21* are localized to the tonoplast.  
82 We show that these proteins regulate meristem size, phyllotaxis, and plant growth, revealing complex  
83 redundant activity within this sub-family and providing a demonstration of the power of the Multi-Knock  
84 approach to discover new biological functions.

85

## 86 **Results**

### 87 **Design of a multi-targeted, CRISPR-based, genome-scale genetic toolbox**

88 The high similarity in coding sequences within plant gene families often results in complete, partial, or  
89 conditional functional redundancy, leading to substantial phenotypic buffering. To construct a genome-  
90 scale library of sgRNAs that would potentially target multiple members from the same family, all gene  
91 families in the *Arabidopsis* genome (TAIR10), encompassing 27,416 protein-coding genes, were  
92 downloaded from the PLAZA 3.0 plant comparative genomics database<sup>24</sup>. Following the filtration of  
93 mitochondrial and chloroplast genes, as well as singletons (i.e., genes without any family members), 21,798  
94 genes remained, belonging to 3,892 families of size 2 or more. We then designed a set of sgRNAs that  
95 would optimally target multiple members of each gene family while accounting for the similarity among  
96 family members (**Fig. 2a,b**). Specifically, a phylogenetic reconstruction strategy was used to hierarchically  
97 organize each family into a tree structure, such that a homologous subgroup of genes that are more closely  
98 related are placed closer to each other on the tree. The optimal sgRNAs that could most efficiently target



99 multiple members of each subgroup were designed using the CRISPyS algorithm<sup>25</sup>. Since CRISPyS could  
100 potentially design the same sgRNAs for different subgroups of the same family, we considered only one  
101 occurrence of each sgRNA (**Fig. 2c,d**). This procedure resulted in a total of 2,183,722 sgRNAs. Next, we  
102 removed sgRNAs that targeted only a single gene with high efficiency, resulting in 1,101,799 sgRNAs. We  
103 then removed sgRNAs with potential high off-target activity towards unintended *Arabidopsis* coding  
104 regions and filtered sgRNAs with overlapping targets. This resulted in a total of 59,129 sgRNAs targeting  
105 16,152 genes (~74% of all protein-coding genes that belong to families) (**Fig. 3a, Extended Data 1**). Of  
106 the 59,129 sgRNAs, 98.7% target two to five genes; the rest target six to ten genes (**Fig. 3b**). This procedure  
107 thus created a library of sgRNAs where every sgRNA targets multiple genes, and every gene is targeted by  
108 multiple sgRNAs (**Fig. 3c, Supplementary Figure 1**).

109

### 110 **Construction of multi-targeted CRISPR sub-libraries for specific functional groups**

111 In an effort to increase the flexibility of the Multi-Knock library and enable targeted forward-genetics  
112 screens, the 59,129 sgRNAs were classified into 10 groups according to the protein functions of their  
113 putative target genes<sup>4</sup>, thus creating the following ten sub-libraries: transporters (TRP: 1,123 genes and  
114 5,635 sgRNAs); protein kinases, protein phosphatases, receptors, and their ligands (PKR: 1,190 genes and  
115 6,161 sgRNAs); transcription factors and other RNA and DNA binding proteins (TFB: 2,042 genes and  
116 6,010 sgRNAs); proteins binding small molecules (BNO: 1,443 genes and 5,899 sgRNAs); proteins that  
117 form or interact with protein complexes including stabilizing factors (CSI: 1,399 genes and 4,919 sgRNAs);  
118 hydrolytic enzymes (enzyme classification [EC] class 3), excluding protein phosphatases (HEC: 1,438  
119 genes and 6,215 sgRNAs); metabolic enzymes and enzymes (EC class2) that catalyze transfer reactions  
120 (TEC: 1,041 genes and 4,145 sgRNAs); catalytically active proteins, mainly enzymes (PEC: 1,252 genes  
121 and 4,975 sgRNAs); proteins with diverse functional annotations not found in the other categories (DMF:  
122 1,343 genes and 5,000 sgRNAs); and proteins of unknown function or cannot be inferred (UNC: 3,881  
123 genes and 10,170 sgRNAs) (**Fig. 3d, Supplementary Table 1**).

124 To facilitate the creation of the sub-libraries, adaptors of 38 to 47 nucleotides in length were added that  
125 were unique to each sub-library (**Supplementary Table 2**). We amplified each sub-library using primers  
126 complementary to the specific adaptors and used the Golden Gate method to clone the sgRNA sub-libraries  
127 into the intronized zCas9 vector (pRPS5A:zCas9i). The intronized *Cas9* has 13 introns integrated into the  
128 maize codon-optimized *Cas9*; these introns have a significant positive effect on *Cas9* genome editing  
129 efficiency in *Arabidopsis*<sup>23</sup>.

130 More than  $2.0 \times 10^5$  clones of each sub-library (average coverage of 20-48× per sgRNA) growing on the  
131 selection plates were harvested, and plasmid DNA from each sub-library was isolated. In order to evaluate

132 library quality, each sub-library was deep sequenced in a 150 paired-end mode (PE150). An ideal sgRNA  
133 library should have < 0.5% undetected guides, and a skew ratio of less than 10<sup>26</sup>. The sequencing data  
134 showed that more than 98% of the designed sgRNAs in our libraries were present, with the exception of  
135 sgRNAs in four sub-libraries (PKR, DMF, HEC, and UNC) that exhibited lower coverage percentages  
136 (95.05%, 80.90%, 85.07%, and 71.58% coverage, respectively) (**Fig. 3e**). Importantly, the sgRNAs  
137 frequencies in the sub-libraries showed a narrow bell-shaped distribution (skew < 2) (**Fig. 3e**), indicating  
138 that no individual sgRNA were overly enriched. In addition, the effect of sgRNA cross-contamination  
139 during library construction was evaluated using deep sequencing analysis. The data indicated that all sub-  
140 libraries are highly specific (~99.9%), with the exception of the TEC sublibrary that showed significant  
141 amplification (35%) of sgRNAs from CSI sublibrary (**Supplementary Figure 2**). With the exception of  
142 the TEC sublibrary, all quality control analyses indicate that the Multi-Knock CRISPR sub-libraries are  
143 ready to be used in plants for functional analysis.

144

#### 145 **Multi-targeted transportome analysis**

146 To demonstrate that the Multi-Knock approach overcomes redundancy in forward-genetics screens *in*  
147 *planta*, we chose to focus on the plant transportome using the TRP sub-library. Transporter families in  
148 plants are generally large (e.g., 136 ABC members and 53 NPF members) and relatively uncharacterized  
149 genetically<sup>27</sup>. To expand the functional utility of our tool, we cloned the 5,635 sgRNA sequences into four  
150 different Cas9 vectors to create independent TRP-sub-libraries, varying in their Cas9 type, the promoter driving  
151 the Cas9, and resistance in plants: pRPS5A:zCas9i library described above, which results in high Cas9 genome-  
152 editing activity in *Arabidopsis*<sup>23</sup>; pRPS5A:Cas9 with OLE:CITRINE that carries BASTA resistance and allows  
153 selection of Cas9 in seeds using a fluorescent Citrine protein<sup>28</sup> (**Supplementary Figure 3**); the commonly used  
154 pUBI:Cas9 also imparts BASTA resistance<sup>29,30</sup>; and pEC:Cas9 that carries kanamycin resistance and allows  
155 mutation specifically in the egg cells to avoid somatic mutations<sup>31</sup>. The four sub-libraries were cloned and deep-  
156 sequenced to evaluate sgRNA coverage and frequency. Coverage was higher than 98%, with a Gaussian  
157 distribution for all four libraries (skew < 3) (**Fig. 4a**).

158 At least 2.2 x 10<sup>5</sup> *Agrobacterium tumefaciens* clones of each TRP-sub-library were harvested and transformed into  
159 *Arabidopsis* Col-0 plants yielding about 3,500 transgenic T1 plants (pUBI:Cas9, 500 lines; pEC:Cas9, 500 lines;  
160 pRPS5A:Cas9 OLE:CITRINE, 500 lines; and pRPS5A:zCas9i 2,000 lines). To increase on-target mutagenesis  
161 in plants, pUBI:Cas9, pEC:Cas9, and pRPS5A:zCas9i T1 plants were subjected to repeated mild heat stress  
162 as previously described with slight modifications<sup>32</sup>. 2,000 T1 lines were collected individually for the  
163 pRPS5A:zCas9i library. pUBI:Cas9, pEC:Cas9, and pRPS5A:Cas9 OLE:CITRINE libraries were each collected  
164 in bulks of 10 plants. 1,200 independent T2 lines generated from the pRPS5A:zCas9i TRP sub-library were

165 screened in soil at 22°C under long-day conditions (16-h light and 8-h dark) using a high-throughput phenomics  
166 system, evaluating photosynthesis-related parameters, thermal imaging, plant color, and shoot morphology.  
167 Importantly, the screen recovered previously reported phenotypes of mutants affected in transporters. For  
168 example, we isolated two independent lines with pale, bleached, and small-size shoots. Extracting DNA,  
169 amplifying the sgRNA cassette, and sequencing revealed that they harbor the same sgRNA sequence,  
170 putatively targeting *TOC132* and *TOC120* (Translocon Outer Complex proteins) (**Fig. 4b, Supplementary**  
171 **Figure 4a**). Sanger sequencing of *TOC132* and *TOC120* revealed that frameshift mutations occurred at the  
172 sgRNA target sites in these two genes (**Fig. 4b, Supplementary Figure 4b**). The similar phenotypes we  
173 observed in two independent lines indeed mimicked the *toc132,toc120* double mutant phenotype that was  
174 previously characterized<sup>33</sup>. In addition, we identified phenotypes driven by two different sgRNAs targeting  
175 two maltose transporters (MEX1 and MEX1-Like). The *mex1,mex1l* CRISPR double mutants phenotype  
176 was enhanced compared to the previously described *mex1* single mutant<sup>34</sup> (**Fig. 4b, Supplementary Figure**  
177 **5**). Plants targeting genes encoding two boron transporters (BOR1 and BOR2) were genotyped as double  
178 *bor1,bor2* knockouts and had growth inhibition phenotypes (**Fig. 4b**), likely enhancing the *bor1-1* mutant-  
179 plants<sup>35</sup>. Unlike all other lines described here which were validated in T2 or T3 generations, the T1  
180 generation *bor1,bor2* knockouts were sterile and did not produce seeds. Sequencing the sgRNA and their  
181 putative target genes of additional lines showed edited DNA events in the majority of the targeting sites  
182 (**Supplementary Figure 6**).

183 Many of the phenotypes we observed were driven by previously undescribed genes. For example, plants  
184 expressing a single sgRNA resulted in deletions in *clc-a*, *clc-b* (Chloride Channels), or *vha-d1*, *vha-d2*  
185 (Vacuolar-type H<sup>+</sup>-ATPases) or *pup8*, *pup21* (Purin Permeases), all showing smaller rosette size than Col-  
186 0 plants (**Fig. 4c**). Notably, while some of the mutations were homozygous, *TOC120*, *VHA-D2*, and *PUP8*  
187 showed superimposed sequencing data. Chromatogram sequence deconvolution showed that *PUP8* is a  
188 biallelic mutation (+T/+A) (**Fig. 4**). The data for *TOC120* and *VHA-D2* is less clear and could point to  
189 biallelic or heterozygous mutations. At this stage, we do not know whether the phenotypes are a result of  
190 an on-target activity, and further genetic validation is needed to rule out off-target effects. Such genetic  
191 validation was carried out below for the *PUP* candidates. Notably, the Multi-Knock seed collection we  
192 generated here is available to the community for any type of forward-genetic screen. Together, the results  
193 demonstrate the strength of the Multi-Knock strategy in exposing novel mutant phenotypes.

194

195 **The Multi-Knock screen revealed partially redundant tonoplast-localized PUP cytokinin**  
196 **transporters**

197 As noted above, the Multi-Knock transportome-scale screen identified a shoot growth inhibition phenotype  
198 caused by *PUP8* and *PUP21* loss-of-function (**Fig. 4c**). The two unstudied proteins are members of the  
199 PUP family, which consists of 21 genes (**Fig. 5a**). Most of the genes in the *PUP Arabidopsis* family have  
200 not been characterized<sup>36</sup>, but *PUP14* reportedly encodes for a plasma membrane cytokinin transporter<sup>37</sup>. In  
201 addition to plasma membrane-localized *PUP14*<sup>37</sup>, *PUP1* and *PUP2* were also identified as cytokinin  
202 transporters in *Arabidopsis*<sup>38,39</sup>. In rice, OsPUP1 and OsPUP7 were shown to localize on the endoplasmic  
203 reticulum (ER), while OsPUP4 was localized to the plasma membrane<sup>40,41</sup>. Cytokinins are plant hormones  
204 essential for meristem maintenance and additional physiological and developmental processes, such as cell  
205 division, lateral root formation, leaf senescence, embryo development and adaptive responses to heat and  
206 drought stresses<sup>42-44</sup>. Because cytokinin biosynthesis, catalyzed by isopentenyl-transferases, does not occur  
207 throughout the plant but is limited to certain tissues, cytokinins are translocated through the plant by  
208 diffusion and/or through active transport mechanisms<sup>36,45</sup>. There is a complete genetic linkage between the  
209 *PUP7*, *PUP21*, and *PUP8* genes, and phylogenetic analysis of *PUPs* in *Arabidopsis* showed that these three  
210 genes form a monophyletic clade (**Fig. 5a**). Similar to *PUP8* and *PUP21*, the function of *PUP7* is unknown.

211 To characterize the activity of *PUP7*, *PUP21*, and *PUP8*, we isolated single *PUP7*, *PUP21*, and *PUP8* T-  
212 DNA homozygous lines. The single *pup7* (SALK\_084103) and *pup8* (SALK\_137526) mutants showed no  
213 morphological differences compared to Col-0. The *pup21* (GABI\_288E11) mutant also did not show a  
214 phenotype in the vegetative stage compared to Col-0, and presented only a mild plant height phenotype after  
215 bolting (**Supplementary Figure 7**). To validate the potentially redundant on-target activity of *PUP7*,  
216 *PUP21*, and *PUP8* as revealed by the *PUP8* and *PUP21* loss-of-function line (**Fig. 4c**), we cloned a  
217 multiplexed CRISPR construct targeting *PUP7*, *PUP21*, and *PUP8* and obtained double (*CRISPR7/21*) and  
218 triple (*CRISPR7/8/21*) mutants. Mutations were validated in generations T4 (*CRISPR7/8/21*) or T3  
219 (*CRISPR7/21*). Both *CRISPR7/21* and *CRISPR7/8/21* showed frameshift mutations in their targets (**Fig.**  
220 **5b**) that exhibited a small rosette size (**Fig. 5c,d**). The phenotype of the triple mutant (*CRISPR7/8/21*) was  
221 enhanced compared to the *CRISPR7/21* double mutant and to the *CRISPR8/21* double mutant recovered  
222 from the Multi-Knock screen (**Fig. 5 c,d**), indicating that *PUP7*, *PUP21*, and *PUP8* redundantly regulate  
223 shoot growth. To further validate the on-target activity of *PUP7*, *PUP21*, and *PUP8* we generated a *PUP7*,  
224 *PUP21*, and *PUP8* multi-targeted amiRNA line (*amiRNA7/8/21*). *amiRNA7/8/21* showed reduced  
225 expression of *PUP7*, *PUP21*, and *PUP8* (**Supplementary Figure 8**). In agreement with the *CRISPR7/8/21*  
226 triple mutant, the *amiRNA7/8/21* line also exhibited a small rosette size (**Fig. 5e,f**).

227 Cytokinin response was previously shown to regulate the spatial distribution of lateral organs along the  
228 stem or phyllotaxis<sup>46</sup>. We found a significant perturbed phyllotaxis phenotype with an increase in the  
229 occurrence of abnormal angles between consecutive organs in *CRISPR7/8/21* and *amiRNA7/8/21* lines

230 (Fig. 5g-j). These results suggest that PUP7, PUP21, and PUP8 redundantly regulate shoot growth and  
231 phyllotaxis.

232 To understand how PUP7, PUP8, and PUP21 function in cellular transport, we generated stable transgenic  
233 plants that express PUP7, PUP8 and PUP21 fused with YFP under the control of the cauliflower mosaic  
234 virus 35S promoter and evaluated the subcellular localization of these proteins in the root meristem  
235 epidermis cells. PUP7 and PUP21 were localized to tonoplasts as indicated by co-localization with the vac-  
236 uole marker<sup>47</sup>, whereas PUP8 localized to the plasma membrane (Fig. 6a). We then performed  
237 transport assays with the 3 proteins in *Xenopus laevis* oocytes using the cytokinin *trans*-zeatin (tZ). Based  
238 on standard import assays and injection-based export assays, PUP8 was shown to be capable of bidirectional  
239 cytokinin transport along the concentration gradient of cytokinin (Fig. 6b,c, Supplementary Figure 9).  
240 The absence of transport activity of PUP7 and PUP21 in oocytes, which do not have vacuoles, likely results  
241 from their mis-localization. In order to back up the oocyte data in a plant system, we expressed all three PUP  
242 transporters in tobacco protoplasts and quantified tZ export after diffusion-based loading. Expression of  
243 *PUP7* and *PUP21* resulted in significantly reduced cellular tZ export, while *PUP8* expression resulted in  
244 enhanced tZ export (Fig. 6d,e). In order to demonstrate substrate specificity, we performed competition  
245 experiments for PUP8 that allowed as a putative tZ exporter for direct competition of tZ uptake into  
246 microsomal fractions. Addition of an excess of cold tZ significantly reduced transport activity of  
247 radiolabelled tZ (Supplementary Figure 10).

248 To evaluate whether these PUP proteins are implicated in cytokinin transport and signaling, we monitored  
249 the shoot apical meristem cytokinin response in Col-0 and *amiRNA7/8/21* plants using the synthetic  
250 cytokinin-inducible reporter *TCS:Venus*<sup>48</sup>. A severely reduced TCS signal was detected in *amiRNA7/8/21*  
251 vegetative and inflorescence shoot apical meristems compared to controls (Fig. 6f-i). The TCS domain at  
252 the center of the SAM and in flowers was also much narrower in *amiRNA7/8/21* compared to wild type  
253 (Fig. 6f,g), thus demonstrating also a change in the spatial distribution of cytokinin responses in the SAM.  
254 Overall, these results indicated that tonoplast-localized PUP7 and PUP21 can act as vacuolar cytokinin  
255 importers, while plasma membrane-localized PUP8 is required for cytokinin export. This cytokinin  
256 transport activity is required to establish the spatial pattern of cytokinin signaling within the SAM, thus  
257 regulating shoot growth and phyllotaxis. However, since directional transport activity of PUP8, and  
258 possibly of PUP7 and PUP21, depends on cytoplasmic (or apoplastic) cytokinin levels, it is possible that  
259 their transport directionality might change spatially. Taken together, our discovery of these novel cytokinin  
260 transporters was made possible through the simultaneous targeting of the multiple *PUP* genes.

261

262 **Discussion**

263 The large number of gene families in *Arabidopsis* results in high levels of functional redundancy<sup>49</sup>. In recent  
264 years, genome-scale amiRNA collections have been developed in *Arabidopsis* and used for forward-genetic  
265 screening to identify hidden phenotypes masked by redundant homologous genes<sup>4,9</sup>. However, this strategy  
266 generally results in incomplete knockout phenotypes. The CRISPR/Cas9 system is a simple, effective  
267 method for generating targeted heritable mutations in the genome and has recently enabled large-scale  
268 knockout mutant libraries of single genes to be generated for forward-genetic screens in mammalian<sup>50,51</sup>  
269 and plant systems<sup>15-19</sup>. An important advantage of the CRISPR/Cas9 method is its capacity to  
270 simultaneously target multiple genes, whether they are genetically linked or not. In this study, we developed  
271 a novel genome-scale approach with the ability to simultaneously target several genes within the same gene  
272 family and applied it in *Arabidopsis*. This forward-genetic strategy overcomes functional redundancy and  
273 enables flexible screening, ranging from a specific functional subgroup to the entire genome. We reported  
274 here on six lines with reproducible phenotypes and validated the respective editing of the target genes. It is  
275 important to note that we have observed dozens of novel phenotypes (i.e., by screening for differences in  
276 shoot size, color, shape and photosynthesis-related parameters) that we have not followed up with detailed  
277 experiments. As the intronized-CAS9 efficiency is above 70%<sup>23,52</sup>, we project that the rate-limiting step is  
278 not the library or the intronized-CAS9 efficiency, but rather the genetic screen setup and cost-effective  
279 genotyping strategies. Overall, the approach we developed and the library we constructed should allow a  
280 broad spectrum of functional screens to be readily carried out, thereby significantly impacting current  
281 genetic analyses in plants.

282 The present strategy constructed the Multi-Knock tool using a single sgRNA design to optimally target  
283 multiple genes. We expect that with the anticipated progress in the field, future developments of the Multi-  
284 Knock approach could utilize sgRNA multiplexing. While constructing a genome-scale sgRNA  
285 multiplexed CRISPR library is at present technically challenging (currently limited by the base-pair length  
286 of pooled oligo libraries containing thousands of sgRNAs), a breakthrough in the field will increase the  
287 overall targeting efficiency and coverage. In addition, the current Multi-Knock tool is designed to target  
288 redundancy resulting from multiple proteins with highly similar sequences carrying overlapping activity  
289 and having highly similar coding sequences. However, Multi-Knock will not reveal redundancy resulting  
290 from overlapping pathways (diverse gene families with overlapping transcriptional or biochemical  
291 activities). The development of a multiplexing Multi-Knock library would naturally uncover redundant  
292 pathways, by allocating each sgRNA to target a different set of (one or more) homologous proteins.

293 As a proof-of-concept that Multi-Knock can identify novel gene functions, we identified the first cytokinin  
294 tonoplast transporters in plants. There are discrepancies in published data concerning the subcellular  
295 localization of cytokinin receptors and the cellular site of cytokinin perception. In different studies,

296 cytokinin receptors have been shown to localize to the endoplasmic reticulum membrane<sup>53-56</sup> and to the  
297 plasma membrane<sup>37</sup>. Recently, two independent groups described multiple sites of cytokinin perception at  
298 plasma and endoplasmic reticulum membranes<sup>57,58</sup>. We speculate that the tonoplast localization of PUP7  
299 and PUP21 may facilitate the movement of cytokinins into vacuoles, thereby lowering the availability of  
300 cytokinins in the cytoplasm and/or the ER. However, it is important to note that injection or diffusion-based  
301 tZ loading might promote PUP-mediated tZ transport from high to low concentration in both *Xenopus* and  
302 tobacco, respectively. Under *in vivo* conditions, it is possible that PUP transport directionalities may also  
303 shift, depending on local cytokinin concentrations or electrochemical gradient changes.

304 The direction of both uni- and symporters was previously shown to be reversible *in vitro* depending on the  
305 direction of the electrochemical gradient of their substrate and/or symported ion<sup>59-62</sup>. For example, PUP8  
306 and the SWEET (SUGARS WILL EVENTUALLY BE EXPORTED TRANSPORTER) transporters were  
307 both identified using import-based screens but were shown to be bidirectional in *Xenopus* oocytes<sup>61,62</sup>.  
308 Lastly, PUP8 was shown to possess phlorizin transport capability via an import-based screen of > 600  
309 *Arabidopsis* transporters and also shown to be bidirectional. Phlorizin is a dihydrochalcone abundantly  
310 found in apples, which indicates that PUP8 might have acquired additional substrates in plants<sup>61</sup>. It is thus  
311 intriguing to speculate that dual-directional PUPs activity in different cell types, possibly among shoot  
312 apical meristem zones, regulates cytokinin response by mediating sub-cellular cytokinin homeostasis. The  
313 tonoplast-dependent cytokinin transport may also have an impact on cell-to-cell cytokinin movement. Such  
314 coordination among a network of plasma membrane and tonoplast transporters might determine the  
315 cytokinin fluxes within the cell and within tissues. Therefore, the tonoplast localization of PUP7 and PUP21  
316 identified here adds another level of regulation to the response mediated by endoplasmic reticulum-  
317 localized cytokinin receptors.

318 Using the Multi-Knock strategy, we demonstrated partially redundant functions of PUP8, PUP7, and  
319 PUP21 in cytokinin transport either across the plasma membrane or into the vacuole, which would both  
320 lead to reduced cytoplasmic cytokinin levels. In all cases, the genes are genetically linked and functionally  
321 redundant, emphasizing the power and need of Multi-Knock as a genome-scale multi-targeted approach. It  
322 is common that evolutionary conserved transporter families in plants share redundant activities and are  
323 genetically linked, suggesting recent gene-duplication events. For example, in five ABCB auxin  
324 transporters (ABCB15-22) of the same phylogenetic branch, their simultaneous knockout using Cas9  
325 exposed their redundant activity<sup>63</sup>. Additional examples are the genetically linked and redundant activities  
326 of ABCB6 and ABCB20 in auxin transport<sup>9</sup> and of ABCG17 and ABCG18 in ABA transport<sup>64</sup>. We predict  
327 that future genetic screens, utilizing approaches as the one developed here, will expose the activities of  
328 many genetically linked and redundant genes.

329 Saturated screens allows to observe the same phenotype in multiple independent lines, creating multiple  
330 alleles and partially omitting false positive candidate lines. Here, we screened ~1,200 independent T2 lines  
331 from the CRISPR TRP library, which contains 5,635 sgRNAs, meaning there is a very low chance of  
332 identifying multiple independent lines containing sgRNAs that target the same genes. However, we  
333 successfully isolated independent lines for *toc120,toc132*, and *mex1,mex11*, likely because of their strong  
334 visible phenotypes. One way to tackle this issue is to screen for high-throughput phenotypes as carried out  
335 in the mammalian field using cell culture<sup>51</sup>. However, such screens do not benefit from the strength of  
336 screening *in planta*. Another way one can isolate multiple events and screen a X10 coverage, saturated  
337 population, is to bulk 10 or 100 lines together (for example, 56K lines covering 5,635 sgRNAs). This allows  
338 rapid screening and increases the chance of identifying the same sgRNA multiple times. At the same time,  
339 this approach has drawbacks as it is harder to pick up on minor phenotypes. An alternative approach to  
340 tackle the issue of saturated screens is to generate smaller libraries that cover specific groups of limited size,  
341 thereby increasing the chance of observing multiple lines directed towards the same set of genes.

342 Following successful phenotyping and genotyping of Multi-Knock T2 plants, just as in any other genetic  
343 approach (e.g., use of alkylating agents, T-DNA, amiRNA), it is critical to validate that the phenotype is  
344 indeed driven by the specific mutation. Ursache et al., reported that an *Agrobacteria* mix, containing  
345 multiple constructs, could result in the integration of more than one construct per plant<sup>52</sup>. Furthermore,  
346 Jacobs et al., reported that transient expression of sgRNAs in tomato might cause CRISPR mediated  
347 mutations in respective target gene<sup>15</sup>, both leading to possible off-target effects. One way to address these  
348 obstacles and reveal possible on/off-targets is to use the SMAP multiplex PCR amplicon tool to genotype  
349 putative target sites<sup>65</sup>. Addition methods to validate on-target activity may include complementation lines  
350 to demonstrate phenotype rescue, or generate multiple independent mutant lines (such as a combination of  
351 T-DNA lines or, in cases of genetic linkage, sgRNAs or amiRNA) that present the same phenotype.

352 Here we presented the Multi-Knock tool and validated its use for gene function discovery in *Arabidopsis*.  
353 This genome-scale multi-targeted mutagenesis system may also be applied to other plant species and  
354 utilized for next-generation breeding programs to uncover hidden genetic variations. However, in contrast  
355 to flower-dip transformation in *Arabidopsis*, large-scale *Agrobacterium*-mediated plant transformations in  
356 crops is still a bottleneck due to low transformation efficiency and the requirement for labor-intensive tissue  
357 culture. Thus, once transformation efficiency is enhanced, for example, using sgRNA delivery by viral  
358 vectors<sup>66,67</sup> or nanoparticle-based carriers<sup>68,69</sup>, we foresee that the Multi-Knock approach could be readily  
359 employed in many other plant species. Notably, the Multi-Knock tool requires high-quality information on  
360 gene space. While high-quality sequenced genomes of most important crops, and dozens of other plants,  
361 are already available, this could be an issue for less studied plant species. A possible alternative in such



362 cases is to extract the gene-space via deep sequencing of the transcriptome, albeit limiting the off-target  
363 search to coding regions only.

364

## 365 **Materials and Methods**

366 **Plant material and growth conditions.** All *Arabidopsis* plants were derived from the Columbia ecotype  
367 and grown in dedicated growth rooms under long-day conditions (16 h light/ 8 h dark) at 22 °C. *Arabidopsis*  
368 Col-0 plants were transformed using *Agrobacterium* strains (GV3101) by the flower dip method<sup>70</sup>.

372 **Multi-targeted sgRNA design.** All 9,350 gene families in the *Arabidopsis thaliana* genome, encompassing  
373 27,416 genes, were downloaded from the PLAZA 3.0 plant comparative genomics database<sup>24</sup>. Genes  
374 belonging to the mitochondrial and chloroplast genomes were filtered out, as well as families with a single  
375 family member, leaving 3,892 families of size 2 or more that together encompassed 21,798 genes. The  
376 CRISPyS algorithm was then applied to each family while accounting for the homologous relationships  
377 within each family. Specifically, given a family of genes, a gene tree was reconstructed using a hierarchical  
378 clustering algorithm<sup>71</sup>, which clusters the genes according to their sequence similarity. The  $s^{\Omega}$  design  
379 strategy of CRISPyS was then recursively applied to each subgroup induced by the gene tree to find the  
380 optimal sgRNAs for targeting the desired subfamily. CRISPyS was applied using the CFD (Cutting  
381 Frequency Determination) score<sup>72</sup> as the scoring function with targeting efficacy threshold of  $\Omega = 0.55$  and  
382  $k = 12$  as the threshold for the number of polymorphic sites. The number of sgRNAs per each subgroup of  
383 genes in a given gene tree was limited to 200. The potential sgRNA targets were allowed only for the first  
384 two-thirds of the coding sequence. Since CRISPyS could assign the same sgRNAs for different subgroups  
385 of homologous genes, where one subgroup is a subset of the other one (for example, assuming that  
386  $\{g_1, g_2, g_3\}$  is a subset of homologous genes, and  $s$  is an sgRNA that targets this subgroup of genes, the  
387 same sgRNA  $s$  can also be found for  $\{g_1, g_2\}$ ), we considered only one occurrence of the sgRNA.

388 For each remaining sgRNA, a genome-wide off-target detection was applied. In the context of gene-family  
389 cleavage, an off-target is defined as a potential genomic target that is outside the specified gene family,  
390 while on-targets are nuclear targets that reside within the family, even though some mismatches may occur  
391 between them and the examined sgRNA. To this end, given a specified sgRNA, the Burrows-Wheeler  
392 Aligner (BWA)<sup>73</sup> was applied to the *Arabidopsis thaliana* genome (PLAZA v3) to identify potential nuclear  
393 hits. BWA was executed with the command "bwa aln", with the following parameters: -N, -l 20, -i 0, -n 5,  
394 -o 0, -d 3, -k 4, -M 0, -O 1000000, -E 0, thus allowing searching for targets with at most four mismatches  
395 and no gaps. Only hits that reside within protein-coding exons were considered off-targets. A potential  
396 sgRNA was filtered if it was inferred to cleave an off-target with a CFD score higher than 0.33. We then  
397 applied an additional filtering procedure, where we tested the remained sgRNAs for overlapping target

398 regions. A given sgRNA was removed if all its targets overlapped with those of a second potential sgRNA,  
399 and the CFD scores of most of these targets were lower. A sgRNA  $s_1$  is defined to overlap with sgRNA  $s_2$   
400 if the positions of all its targets overlap with those of  $s_2$  in at least 10% of the aligned region (i.e., 2 bp).

#### 410 **CRISPR/Cas9 vectors**

411 To generate the pRPS5A:Cas9 OLE:CITRINE plasmid, Site-Directed Mutagenesis (NEB-E0554S), was used to  
412 eliminate the 3 BsaI sites within the OLE:CITRINE sequence, using the following primers: Fwd-  
413 ATGGGCCGAGACAGGGACCAGTACCAGATGTCCGGAC Rev-  
414 CATCGGGTACTGGTCCCTGCCGATGATATCGTGATGG. The BsaI sites are required for the Golden gate  
415 CRISPR library cloning. Next, OLE:CITRINE was cut and ligated from pJET into pRPS5A:Cas9 vector using  
416 MluI and BamHI restriction enzymes. pUBI:Cas9 was generated as described previously<sup>29</sup>. pRPS5A:zCAS9i  
417 (Addgene ID: AGM55261)<sup>23</sup> and pEC:Cas9 (Addgene ID: pHEE401)<sup>31</sup> were purchased from Addgene.

418 **Construction of Multi-Knock, multi-targeted CRISPR libraries.** The 20-nucleotide sgRNA target sites  
419 were appended with the specific adaptors and BsaI sites (**Supplementary Table 2**). Synthesis of the 59,129  
420 DNA oligonucleotides (total yield: 500 ng) corresponding to the sgRNAs was performed by Twist  
421 Bioscience. A stock solution of oligo pool was prepared by resuspending in 10 mM Tris buffer, pH 8.0 to  
422 a concentration of at least 20 ng/ $\mu$ l. The single-stranded oligonucleotide pool was converted to double-  
423 stranded DNA by PCR using the high-fidelity Phusion polymerase (NEB) using 12 to 15 cycles of PCR to  
424 avoid introducing PCR bias. PCR was conducted using the following conditions: 98 °C for 30 s; 15 cycles  
425 of 98 °C for 30 s, 60 °C for 30 s, and 72 °C for 15 s; and a final extension at 72 °C for 10 min. For each  
426 family pool, about 6 tubes of 50  $\mu$ l-volume amplification reactions with a total of 15 ng single-stranded  
427 oligonucleotide pool as a template and the specific primers for adaptors (**Supplementary Table 3**) were  
428 used, and the PCR products were purified with a NucleoSpin Gel and PCR clean up Kit (Macherey-Nagel).

429 The purified DNA products were digested with BsaI restriction enzyme and ligated into the desired Cas9  
430 expression constructs using the Golden Gate cloning method. Golden Gate assembly was performed as  
431 follows: 35 cycles of 37 °C for 5 min and 16 °C for 5 min; 50 °C for 20 min; and 80 °C for 20 min. Four  
432 20- $\mu$ l ligation reactions were combined, and 20 bacterial transformations were carried out using 4  $\mu$ l of  
433 ligation reaction and 50  $\mu$ l Top10 chemically competent *E. coli* per transformation according to the  
434 manufacturer's instructions. The 20 transformations were combined and plated onto seven LB agar plates  
435 (145 x 20 mm, Greiner Bio-one) supplemented with the relevant antibiotics. Colonies were validated using  
436 colony PCR and Sanger sequencing individually, then bacteria from all plates were scraped off and  
437 combined. The plasmid DNA was purified with a Plasmid Maxi kit (Qiagen) to produce the CRISPR  
438 libraries. In order to verify these plasmid pools, PCR products amplified with the primers listed in  
439 **Supplementary Table 4** from the CRISPR libraries were sequenced on an Illumina NovaSeq 6000 with

440 the PE150 mode. Eight 50  $\mu$ l amplification reactions using the high-fidelity Phusion DNA Polymerase  
441 (NEB) were set up. PCR was conducted using the following conditions: 98  $^{\circ}$ C for 30 s; 30 cycles of 98  $^{\circ}$ C  
442 for 30 s, 60  $^{\circ}$ C for 30 s, and 72  $^{\circ}$ C for 15 s; and a final extension at 72  $^{\circ}$ C for 10 min. PCR products were  
443 purified with a NucleoSpin Gel and PCR clean-up Kit (Macherey-Nagel). At least 1.5  $\mu$ g PCR products per  
444 each sub-library were sent to Novogene for deep-sequencing.

445 The number of reads per sgRNA sequence was quantified from the raw sequencing data using the Biopython  
446 package in the Python programming language. A list of sgRNAs comprising the library was loaded into  
447 python. A loop was performed where each one of the sgRNAs in the list was compared against the raw  
448 deep-sequencing data in FASTA using the Biopython package and quantified the number of reads where  
449 the specific sgRNA appeared. The sgRNA and its read number were written into a new data frame.

450 **Generation of four transportome CRISPR libraries.** The four transportome CRISPR plasmids were  
451 transformed into *Agrobacterium tumefaciens* strain GV3101 using electroporation. In brief, for each library,  
452 around 20 tubes of GV3101 competent cells (80  $\mu$ l) were incubated on ice with  $\sim$ 1  $\mu$ g plasmid in each tube  
453 for 5 min and electroporated using a MicroPulser (Bio-Rad Laboratories; 2.2 kV, 5.9 ms). Immediately  
454 after electroporation, 700  $\mu$ l LB medium was added, and samples were shaken for 1.5-2 h at 28  $^{\circ}$ C.  
455 *Agrobacterium* was then plated on LB agar plates (145 x 20 mm, Greiner Bio-one) containing the relevant  
456 antibiotics for 2 days at 28  $^{\circ}$ C in the dark. Each *Agrobacterium* transportome CRISPR library was  
457 transformed into six trays of *Arabidopsis* Col-0 plants. T1 Seeds were collected in bulk. After transformant  
458 plant selection, transgenic plants for each transportome CRISPR library were propagated, and T2 seeds  
459 were collected.

460 ***Arabidopsis* transformation and heat-shock treatment.** The *Agrobacterium* colonies from all plates were  
461 scraped off and added into 1 L LB medium with 25  $\mu$ g/ml gentamycin, 25  $\mu$ g/ml rifampicin, and vector-  
462 specific antibiotic, followed by incubation at 28  $^{\circ}$ C for 16-24 hours. *Agrobacterium* was harvested by  
463 centrifugation for 10 min at 5,500 rpm, the supernatant was discarded, and the bacteria pellet was  
464 resuspended in  $\sim$ 400 ml inoculation medium containing 0.5 x MS (Duchefa Biochemie), 5.0% sucrose, and  
465 0.05% Tween-20 (Sigma-Aldrich). *Arabidopsis* flowers were then sprayed with the bacterial solution. After  
466 spraying, plants were kept in the dark overnight and grown until siliques ripened and dried. T1 seeds were  
467 collected in bulk. The T1 seeds of the pEC:zCas9 library were sown on MS media containing hygromycin  
468 (25  $\mu$ g/ml) for the transformant plant selection, whereas the T1 seeds of the other three transportome  
469 CRISPR libraries were sown on soil and sprayed with BASTA for selection at the age of 2 weeks. T1  
470 transgenic plants were subjected to repeated heat stress treatments as previously described with slight  
471 modifications<sup>32</sup> (with the exception of pRPS5A:Cas9 OLE:CITRINE). The plants that were subjected to  
472 heat stress were treated as follows: After resistance selection and 4 days of acclimation to the soil, the

473 seedlings were transferred to growth chambers at 32 °C for 24 h, followed by a 48 h recovery at 22 °C (3-  
474 day period). This heat stress cycle was performed four times during the vegetative phase of growth. The  
475 plants were then grown at 22 °C from that point on.

476 **CRISPR/CAS9 and amiRNA cloning.** The 20 nt protospacer (CTCTACTTTCTCCCTCATCT) was  
477 picked to target PUP7 (AT4G18197), PUP8 (AT4G18195) and PUP21 (AT4G18205) at once. The oligos  
478 (FW: attgCTCTACTTTCTCCCTCATCT; REV: aaacAGATGAGGGAGAAAGTAGAG) were annealed  
479 and cloned into the pRPS5A:zCAS9i (Addgene: AGM55261) using the Golden Gate cloning method. In  
480 brief, the oligos were incubated at 95°C for 5 mins and cooled at RT for 20 mins. The annealed oligos and  
481 the pRPS5A:zCAS9i were added in the following reaction (20 µl): 3µl of annealed oligos; ~150 ng of CAS9  
482 vector; 1 µl T4 ligase (400,000 units/ml, NEB); 1 µl BsaI-HF v2 (20,000 units/ml, NEB); Cutsmart buffer  
483 (NEB) and T4 ligase buffer (NEB). Golden Gate assembly was performed as follows: 35 cycles of 37 °C  
484 for 5 min and 16 °C for 5 min; 50 °C for 20 min; and 80 °C for 20 min. 1/10 of the reaction was transformed  
485 into *E.coli* DH5α.

486 To generate the 35S:amiRNA-PUP7/8/21 vector, the amiRNA319 backbone sequence with miR targeting  
487 *PUP7*, *PUP8* and *PUP21* (MiR-sense: TATCATGGAAAACACTGTCCTG) was synthesized by Syntezza  
488 Bioscience Ltd. and cloned into the pH2GW7 destination vector using the Gateway system.

489 **Genotyping.** To identify the sgRNA of transgenic plants, genomic DNA from young leaf tissue was  
490 extracted by grinding 1-2 leaves into 400 µl Extraction Buffer (200 mM Tris-HCl, pH 8.0, 250 mM NaCl,  
491 25 mM EDTA, and 0.5% SDS). After 1-min centrifugation at 13,000 rpm, 300 µl supernatant was  
492 transferred to a new Eppendorf tube and mixed with 300 µl isopropanol, followed by centrifugation for 10  
493 min at maximum speed. The supernatant was removed and the DNA pellets were washed with 70% ethanol  
494 and then resuspended in 50 µl of water. The PCR amplified using the primers listed in **Supplementary**  
495 **Table 4 and 5** was identified using Sanger sequencing.

496 T-DNA lines for the single mutants, listed in **Supplementary Table 6**, were ordered from Gabi Kat  
497 (<https://www.gabi-kat.de>) and The *Arabidopsis* Information Resource (<https://www.arabidopsis.org/>).  
498 Primers for the T-DNA genotyping were designed using the T-DNA Primer Design Tool powered by  
499 Genome Express Browser Server (<http://signal.salk.edu/tdnaprimers.2.html>). Homozygous mutants were  
500 selected by PCR performed with primers listed in **Supplementary Table 6**.

501 **Phenomics.** Morphological and photosynthesis parameters were analyzed with the PlantScreen™  
502 Phenotyping System, Photon Systems Instruments (PSI), Czech Republic. Plants were sowed in PSI  
503 standard pots and imaged at day 25.

504 **35S:YFP-PUPs cloning.** PUP7 genomic DNA, PUP8-CDS and PUP21-CDS were amplified with Phusion  
505 High-fidelity Polymerase (NEB) using the primers list in **Supplementary Table 7**. PUP7 genomic  
506 sequence with intron, PUP8, and PUP21 coding regions was cloned into pENTER/D-TOPO (Invitrogen  
507 K2400), verified by sequencing, and subsequently cloned into the binary destination vector (pH7WGY2)  
508 using LR Gateway reaction (Invitrogen 11791). *p35S:YFP-PUP7*, *p35S:YFP-PUP8*, and *p35S:YFP-*  
509 *PUP21* were generated using the pH7WGY2 vector and were selected using spectinomycin in *Escherichia*  
510 *coli* and hygromycin in plants.

511 **Microscopy imaging.** Seedlings were stained in 10 mg L<sup>-1</sup> propidium iodide (PI) for 5 min and rinsed in  
512 water for 30 s. Confocal microscopy was performed using a Zeiss LSM780 inverted confocal microscope  
513 equipped with a 20×/0.8 M27 objective lens. YFP and CFP were excited using an argon-ion laser, whereas  
514 PI was excited using a diode laser. Emissions were detected sequentially with ZEN to prevent crosstalk  
515 between fluorophores. YFP was excited at 514 nm, CFP at 458 nm, and PI at 561 nm. Fluorescence emission  
516 was measured at 517-561 nm (YFP), 523-552 (CITRINE), 463-517 nm (CFP), and 588-718 nm (PI).

517 **Expression and cytokinin transport assays in *Xenopus* oocytes.** Coding DNA sequences of PUP7, PUP8  
518 and PUP21 were cloned into *Xenopus laevis* oocyte expression vector pNB1u using USER cloning  
519 technique as described previously<sup>74</sup>. DNA template for in vitro transcription was generated by PCR using  
520 Phusion High-Fidelity DNA Polymerase (NEB) using forward primer (5'-  
521 AATTAACCCTCACTAAAGGGTTGTAATACGACTCACTATAGGG-3') and reverse primer (5'-  
522 TTTTTTTTTTTTTTTTTTTTTTTTTTTTATACTCAAGCTAGCCTCGAG-3'). The PCR products  
523 were purified using the E.Z.N.A. Cycle Pure Kit (Omega Bio-tek). Capped complementary RNA (cRNA)  
524 was in vitro transcribed using the mMessage mMachine T7 Kit (Invitrogen AM1344) following the  
525 manufacturer's instructions.

526 *X. laevis* oocytes (stage V or VI) were purchased from Ecocyte Bioscience (Germany). Oocytes were  
527 injected with 15 ng of PUP7, PUP8, or PUP21 cRNA (or 50.6 nl nuclease-free water as mock control) using  
528 a Drummond NANOJECT II (Drummond Scientific Company, Broomall Pennsylvania). The injected  
529 oocytes were incubated for 3 days at 16°C in a kulori buffer (90 mM NaCl, 1 mM KCl, 1 mM MgCl<sub>2</sub>, 1  
530 mM CaCl<sub>2</sub>, 5 mM Hepes pH 7.4) supplemented with gentamycin (100 µg/ml).

531 Three days after cRNA injection, the injection-based export assay was performed. Oocytes were injected  
532 with 23nl of 2mM trans-zeatin (tZ) and then oocytes were incubated in a group of 3 oocytes in 150 ul kulori  
533 buffer (90 mM NaCl, 1 mM KCl, 1 mM MgCl<sub>2</sub>, 1 mM CaCl<sub>2</sub>, 10 mM MES pH 5.5) for 150 min. After  
534 150 min, the oocytes and their respective external medium were harvested separately for intracellular and  
535 extracellular tZ quantification, respectively. The samples were homogenized with 50% methanol and then  
536 stored at -20°C overnight. Subsequently, the extracts were spun down at 15,000g for 15 min at 4°C and the

537 supernatant was diluted with water, filtered through a 0.22 µm polyvinylidene difluoride-based filter plate  
538 (MSGVN2250, Merck Millipore), and analyzed by analytical liquid chromatography coupled to mass  
539 spectrometry (LC-MS/MS). Export of tZ was calculated as follows: ((amount of tZ in the medium at time  
540 t=150 min)/(amount of tZ in the oocyte at time t=150 min + amount of tZ in the medium at time t=150  
541 min))\*100%.

542 Uptake assay was performed as described previously<sup>75</sup>, with some modifications. A mixture of three types  
543 of cytokinin (*trans*-zeatin (tZ), *trans*-zeatin riboside (tZR), and isopentenyl adenosine (iPR)) with a final  
544 concentration of each type at 10 or 100 µM were used. Three days after cRNA injection, oocytes were  
545 preincubated in kulori buffer (pH 5.5 or pH 8.5) for five minutes, and then the oocytes were incubated in  
546 10 or 100 µM of cytokinin mix (tZ, tZR and iPR) containing kulori buffer (pH 5.5 or pH 8.5) for 60 min.  
547 Oocytes were then washed four times in kulori buffer (pH 5.5 or pH 8.5) and homogenized with 50 %  
548 methanol. Subsequent extraction and oocyte sample preparation was performed as described above.

549 **Cytokinin quantification by LC-MS/MS.** Samples were 100-fold diluted with deionized water and  
550 subjected to analysis by liquid chromatography coupled to mass spectrometry. Chromatography was  
551 performed on an Advance UHPLC system (Bruker, Bremen, Germany). Separation was achieved on a  
552 Kinetex 1.7u XB-C18 column (100 x 2.1 mm, 1.7 µm, 100 Å, Phenomenex, Torrance, CA, USA). Formic  
553 acid (0.05%) in water and acetonitrile (supplied with 0.05% formic acid) were employed as mobile phases  
554 A and B, respectively. The elution profile was: 0-0.1 min, 5% B; 0.1-1.0 min, 5-45 % B; 1.0-3.0 min 45-  
555 100 % B, 3.0-3.5 min 100 % B, 3.5-3.55 min, 100-5 % B and 3.55-4.7 min 5 % B. The mobile phase flow  
556 rate was 400 µl min<sup>-1</sup>. The column temperature was maintained at 40°C. The liquid chromatography was  
557 coupled to an EVOQ Elite TripleQuadrupole mass spectrometer (Bruker, Bremen, Germany) equipped with  
558 an electrospray ion source (ESI). The instrument parameters were optimized by infusion experiments with  
559 pure standards. The ion spray voltage was maintained at +5000 V in positive mode. Cone temperature was  
560 set to 350 °C and cone gas to 20 psi. The heated probe temperature was set to 250 °C and probe gas flow  
561 to 50 psi. Nebulizing gas was set to 60 psi and collision gas to 1.6 mTorr. Nitrogen was used as a probe and  
562 nebulizing gas and argon as collision gas. The active exhaust was constantly on. Multiple reaction  
563 monitoring (MRM) was used to monitor analyte precursor ion → fragment ion transitions. MRM transitions  
564 were adapted from literature<sup>76</sup>. Detailed values for mass transitions and references are listed in  
565 **Supplementary Table 8.** Both Q1 and Q3 quadrupoles were maintained at unit resolution. Bruker MS  
566 Workstation software (Version 8.2.1, Bruker, Bremen, Germany) was used for data acquisition and  
567 processing. Linearity in ionization efficiencies were verified by analyzing dilution series.

568 **Tobacco cytokinin transport assays.** For protoplast export experiments, *35S:YFP:PUPs* were transiently  
569 expressed in *N. benthamiana* leaf tissues by *Agrobacterium tumefaciens*-mediated transfection, protoplasts  
570 were prepared and [<sup>14</sup>C]*tZ* and [<sup>3</sup>H]BA export was quantified simultaneously as described previously<sup>77</sup>.  
571 For microsomal uptake experiments, *35S:YFP:PUP8* was expressed in *N. benthamiana* leaf tissue by  
572 *Agrobacterium tumefaciens*-mediated transfection, and microsomes were prepared and assayed as  
573 described previously<sup>37</sup>. In short, <sup>14</sup>C-labelled *tZ* was added to 300 µg of 25 microsomes in the presence of  
574 5 mM ATP to yield a final concentration of 1 µM [<sup>14</sup>C]*tZ*. For substrate competition assays, unlabelled  
575 substrate was included in the transport buffer at a 100-fold excess. After 10 s of incubation at 20°C, aliquots  
576 of 100 µl were vacuum-filtered and subjected to scintillation counting. Means and standard error of means  
577 of at least four independent experiments with four technical replicates each are represented.

578 **Measurements of *TCS:Venus* responses.** Leaf or floral primordia were removed with the help of a fine  
579 forceps (Swiss No.5) under a Nikon SMZ 745 stereoscope. Dissected shoot apices were inserted into Apex  
580 Culture Medium (1/2 x MS medium (Duchefa), 1% sucrose, 1% agarose, 2 mM MES (Sigma), 1x vitamin  
581 solution (myo-Inositol 100 mg/L, nicotinic acid 1 mg/L, pyridoxine hydrochloride 1 mg/L, thiamine  
582 hydrochloride 10 mg/L, glycine 2 mg/L), 250 nM N6-Benzyladenine)). Confocal images were obtained  
583 with a Zeiss LSM 700 microscope equipped with a water-dipping lens (W Plan-Apochromat 40x/1.0 DIC).  
584 Venus and auto-fluorescence (chlorophyll A) were excited by both 488 nm laser with emission range at  
585 300-550 nm and 664-800 nm, respectively. Images were processed and analyzed using Fiji (fiji.sc)  
586 software.

587 **Phylogenetic tree.** A phylogenetic tree of *Arabidopsis* PUP family members, based on protein sequences,  
588 was constructed using Phylogeny.fr (<http://www.phylogeny.fr/>)<sup>78</sup> with “one-click” mode. The previously  
589 unreported PUP9 protein (AT4G18220), a close paralog of PUP10, was identified and added to the  
590 phylogenetic analysis (**Fig. 5a**).

591 **Measurements of silique divergence angles.** Angles separating successive siliques on the main  
592 inflorescence stem were quantified using a protractor as previously described<sup>79</sup>. The divergence angle was  
593 measured between the insertion points of two successive floral pedicels. Phyllotaxy orientation can be either  
594 clockwise or anticlockwise.

595

## 596 **Acknowledgments**

597 We thank Bruno Müller (University of Zurich, Switzerland) for sharing *TCS:VENUS* seeds. **Funding:** This  
598 work was supported by grants from the Israel Science Foundation (2378/19 and 3419/20 to E.S.), the  
599 Human Frontier Science Program (HFSP—RGY0075/2015 and HFSP—LIY000540/2020 to E.S., H.H.N.-

600 E. and Z.M.B.), Danmarks Grundforskningsfond (DNRF99 to H.H.N.-E.), the European Research Council  
601 (757683-RobustHormoneTrans to E.S.), the PBC postdoctoral fellowship (to Y.H.), and by the Swiss  
602 National Funds (31003A-165877/1 to M.G.).

603

#### 604 **Author contributions**

605 Y.H. and E.S. conceived and designed the study and wrote the manuscript. Y.H. performed the research.  
606 P.P. assisted in cloning the Multi-Knock libraries and with PUP genetics. O.P. cloned and characterized the  
607 PUP amiRNA and PUP reporter lines. A.S., G.H. and O.C. carried out the Multi-Knock sgRNA library  
608 bioinformatics design and analysis. Z.M.B. performed transport assays in the *Xenopus* oocytes. J.B. carried  
609 out the Multi-Knock sgRNA library deep-sequencing analysis. S.B. cloned the OLE:CITRINE Cas9 vector.  
610 B.S. carried out the *TCS:VENUS* assays. L.C. performed the tobacco transport assays. C.C. performed the  
611 LC-MS analysis. Y.Z. assisted in the PUP genes discovery. M.T. assisted in the library screen. D.W assisted  
612 in the Multi-Knock sgRNA library design. A.A. provided the UBI:Cas9 vector. H.H.N.-E., M.G., T.V., and  
613 I.M. designed and supervised the work and edited the manuscript. All authors discussed the results and  
614 commented on the manuscript.

615

616 **Competing interests:** The authors declare that they have no competing interests.

617

618 **Data, code and materials availability:** All the data and supporting the findings of this study are available  
619 within the article and the Supplementary Materials. All source codes used to generate the library are  
620 available upon request.

621

#### 622 **References**

- 623 1. Panchy, N., Lehti-Shiu, M. & Shiu, S. H. Evolution of gene duplication in plants. *Plant Physiol.*  
624 **171**, 2294–2316 (2016).
- 625 2. Rensing, S. A. Gene duplication as a driver of plant morphogenetic evolution. *Curr. Opin. Plant*  
626 *Biol.* **17**, 43–48 (2014).
- 627 3. Alonso, J. M. *et al.* Genome-wide insertional mutagenesis of *Arabidopsis thaliana*. *Science.* **301**,  
628 653–657 (2003).
- 629 4. Hauser, F. *et al.* A genomic-scale artificial MicroRNA library as a tool to investigate the  
630 functionally redundant gene space in *Arabidopsis*. *Plant Cell* **25**, 2848–2863 (2013).
- 631 5. Henry, I. M. *et al.* Efficient genome-wide detection and cataloging of EMS-induced mutations  
632 using Exome capture and next-generation sequencing. *Plant Cell* **26**, 1382–1397 (2014).
- 633 6. Tal, I. *et al.* The *Arabidopsis* NPF3 protein is a GA transporter. *Nat. Commun.* **7**, 11486 (2016).

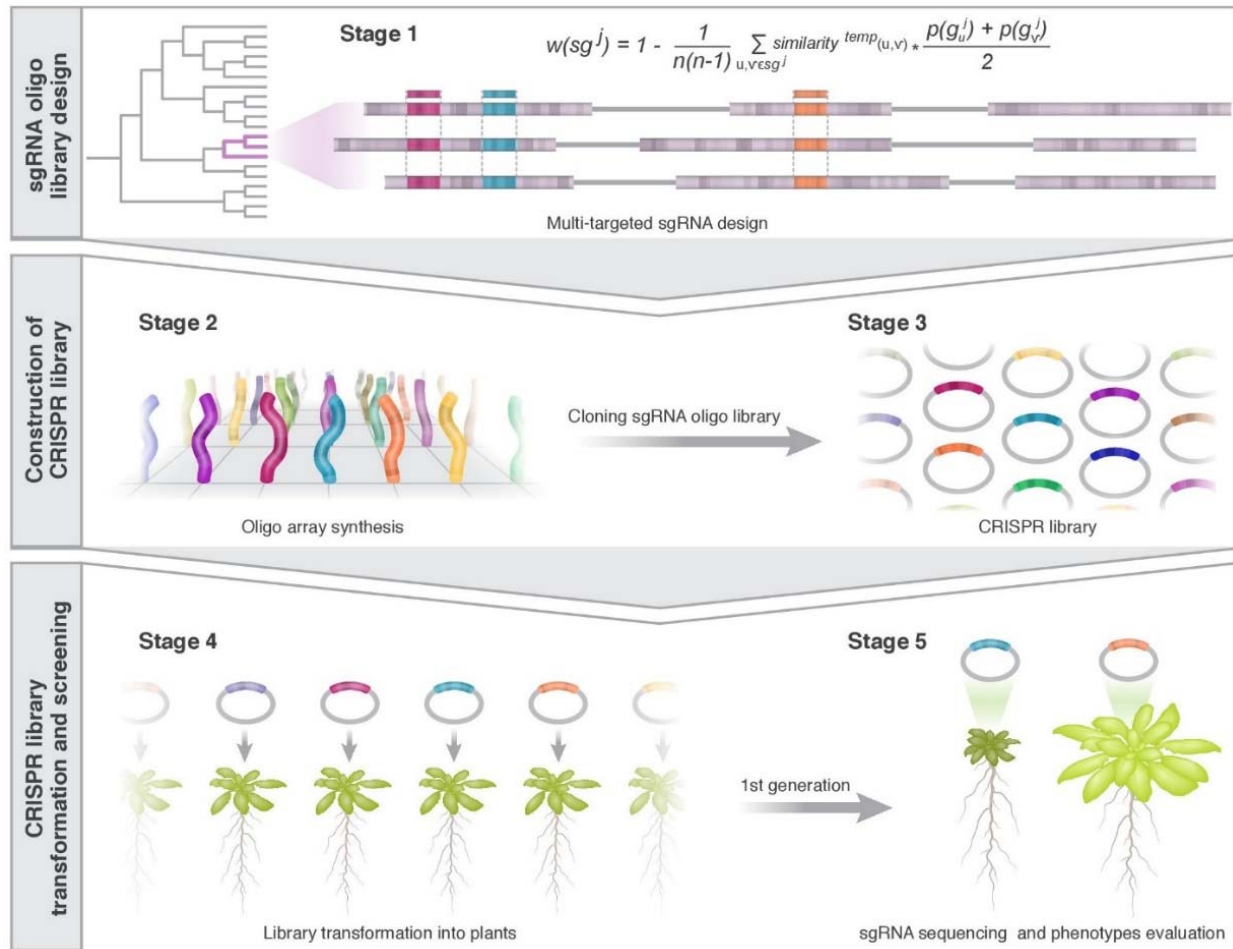


- 634 7. Tang, X. *et al.* A Single Transcript CRISPR-Cas9 System for Efficient Genome Editing in Plants.  
635 *Mol. Plant* **9**, 1088–1091 (2016).
- 636 8. Wang, L. *et al.* Construction of a genomewide RNAi mutant library in rice. *Plant Biotechnol. J.*  
637 **11**, 997–1005 (2013).
- 638 9. Zhang, Y. *et al.* A transportome-scale amiRNA-based screen identifies redundant roles of  
639 Arabidopsis ABCB6 and ABCB20 in auxin transport. *Nat. Commun.* **9**, 4204 (2018).
- 640 10. Li, Z. *et al.* Gene duplicability of core genes is highly consistent across all angiosperms. *Plant Cell*  
641 **28**, 326–344 (2015).
- 642 11. Lu, X. *et al.* Gene-Indexed Mutations in Maize. *Mol. Plant* **11**, 496–504 (2018).
- 643 12. Gaillochet, C., Develtere, W. & Jacobs, T. B. CRISPR screens in plants: Approaches, guidelines,  
644 and future prospects. *Plant Cell* **33**, 794–813 (2021).
- 645 13. Chen, K., Wang, Y., Zhang, R., Zhang, H. & Gao, C. CRISPR/Cas Genome Editing and Precision  
646 Plant Breeding in Agriculture. *Annu. Rev. Plant Biol.* **70**, 667–697 (2019).
- 647 14. Mali, P. *et al.* RNA-guided human genome engineering via Cas9. *Science.* **339**, 823–826 (2013).
- 648 15. Jacobs, T. B., Zhang, N., Patel, D. & Martin, G. B. Generation of a collection of mutant tomato  
649 lines using pooled CRISPR libraries. *Plant Physiol.* **174**, 2023–2037 (2017).
- 650 16. Chen, K. *et al.* A FLASH pipeline for arrayed CRISPR library construction and the gene function  
651 discovery of rice receptor-like kinases. *Mol. Plant* **15**, 243–257 (2021).
- 652 17. Liu, H. J. *et al.* High-throughput CRISPR/Cas9 mutagenesis streamlines trait gene identification in  
653 maize. *Plant Cell* **32**, 1397–1413 (2020).
- 654 18. Lu, Y. *et al.* Genome-wide Targeted Mutagenesis in Rice Using the CRISPR/Cas9 System. *Mol.*  
655 *Plant* **10**, 1242–1245 (2017).
- 656 19. Meng, X. *et al.* Construction of a Genome-Wide Mutant Library in Rice Using CRISPR/Cas9.  
657 *Mol. Plant* **10**, 1238–1241 (2017).
- 658 20. Bai, M. *et al.* Generation of a multiplex mutagenesis population via pooled CRISPR-Cas9 in soya  
659 bean. *Plant Biotechnol. J.* **18**, 721–731 (2020).
- 660 21. Ramadan, M. *et al.* Efficient CRISPR/Cas9 mediated Pooled-sgRNAs assembly accelerates  
661 targeting multiple genes related to male sterility in cotton. *Plant Methods* **17**, 1–13 (2021).
- 662 22. Lorenzo, C. D. *et al.* BREEDIT: a multiplex genome editing strategy to improve complex  
663 quantitative traits in maize. *Plant Cell* (2022).
- 664 23. Grützner, R. *et al.* High-efficiency genome editing in plants mediated by a Cas9 gene containing  
665 multiple introns. *Plant Commun.* **2**, 1–15 (2021).
- 666 24. Proost, S. *et al.* PLAZA 3.0: An access point for plant comparative genomics. *Nucleic Acids Res.*  
667 **43**, D974–D981 (2015).
- 668 25. Hyams, G. *et al.* CRISPyS: Optimal sgRNA Design for Editing Multiple Members of a Gene  
669 Family Using the CRISPR System. *J. Mol. Biol.* **430**, 2184–2195 (2018).
- 670 26. Joung, J. *et al.* Genome-scale CRISPR-Cas9 knockout and transcriptional activation screening.  
671 *Nat. Protoc.* **12**, 828–863 (2017).

- 672 27. Kang, J. *et al.* Plant ABC Transporters. *Arab. B.* **9**, e0153 (2011).
- 673 28. Tsutsui, H. & Higashiyama, T. PKAMA-ITACHI vectors for highly efficient CRISPR/Cas9-  
674 mediated gene knockout in *Arabidopsis thaliana*. *Plant Cell Physiol.* **58**, 46–56 (2017).
- 675 29. Sussholz, O., Pizarro, L., Schuster, S. & Avni, A. SIRLK-like is a malectin-like domain protein  
676 affecting localization and abundance of LeEIX2 receptor resulting in suppression of EIX-induced  
677 immune responses. *Plant J.* **104**, 1369–1381 (2020).
- 678 30. Fauser, F., Schiml, S. & Puchta, H. Both CRISPR/Cas-based nucleases and nickases can be used  
679 efficiently for genome engineering in *Arabidopsis thaliana*. *Plant J.* **79**, 348–359 (2014).
- 680 31. Wang, Z. P. *et al.* Egg cell-specific promoter-controlled CRISPR/Cas9 efficiently generates  
681 homozygous mutants for multiple target genes in *Arabidopsis* in a single generation. *Genome Biol.*  
682 **16**, 1–12 (2015).
- 683 32. LeBlanc, C. *et al.* Increased efficiency of targeted mutagenesis by CRISPR/Cas9 in plants using  
684 heat stress. *Plant J.* **93**, 377–386 (2018).
- 685 33. Kubis, S. *et al.* Functional specialization amongst the *Arabidopsis* Toc159 Family of chloroplast  
686 protein import receptors. *Plant Cell* **16**, 2059–2077 (2004).
- 687 34. Niittylä, T. *et al.* A Previously Unknown Maltose Transporter Essential for Starch Degradation in  
688 Leaves. *Science.* **303**, 87–89 (2004).
- 689 35. Takano, J. *et al.* *Arabidopsis* boron transporter for xylem loading. *Nature* **420**, 337–340 (2002).
- 690 36. Kang, J., Lee, Y., Sakakibara, H. & Martinoia, E. Cytokinin Transporters: GO and STOP in  
691 Signaling. *Trends Plant Sci.* **22**, 455–461 (2017).
- 692 37. Zürcher, E., Liu, J., Di Donato, M., Geisler, M. & Müller, B. Plant development regulated by  
693 cytokinin sinks. *Science.* **353**, 1027–1030 (2016).
- 694 38. Bürkle, L. *et al.* Transport of cytokinins mediated by purine transporters of the PUP family  
695 expressed in phloem, hydathodes, and pollen of *Arabidopsis*. *Plant J.* **34**, 13–26 (2003).
- 696 39. Gillissen, B. *et al.* A new family of high-affinity transporters for adenine, cytosine, and purine  
697 derivatives in *Arabidopsis*. *Plant Cell* **12**, 291–300 (2000).
- 698 40. Xiao, Y. *et al.* Endoplasmic Reticulum-Localized PURINE PERMEASE1 Regulates Plant Height  
699 and Grain Weight by Modulating Cytokinin Distribution in Rice. *Front. Plant Sci.* **11**, 1–12  
700 (2020).
- 701 41. Xiao, Y. *et al.* Big Grain3, encoding a purine permease, regulates grain size via modulating  
702 cytokinin transport in rice. *J. Integr. Plant Biol.* **61**, 581–597 (2019).
- 703 42. Perilli, S., Moubayidin, L. & Sabatini, S. The molecular basis of cytokinin function. *Curr. Opin.*  
704 *Plant Biol.* **13**, 21–26 (2010).
- 705 43. Wybouw, B. & De Rybel, B. Cytokinin – A Developing Story. *Trends Plant Sci.* **24**, 177–185  
706 (2019).
- 707 44. Ha, S., Vankova, R., Yamaguchi-Shinozaki, K., Shinozaki, K. & Tran, L. S. P. Cytokinins:  
708 Metabolism and function in plant adaptation to environmental stresses. *Trends Plant Sci.* **17**, 172–  
709 179 (2012).
- 710 45. Sakakibara, H. Cytokinins: Activity, biosynthesis, and translocation. *Annu. Rev. Plant Biol.* **57**,

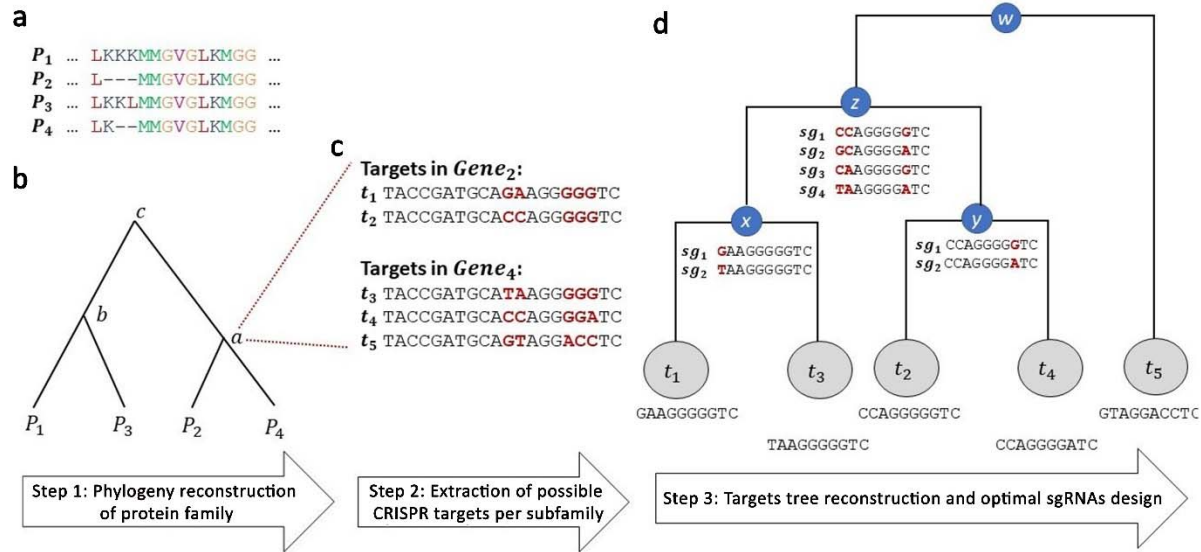
- 711 431–449 (2006).
- 712 46. Besnard, F. *et al.* Cytokinin signalling inhibitory fields provide robustness to phyllotaxis. *Nature*  
713 **505**, 417–421 (2014).
- 714 47. Nelson, B. K., Cai, X. & Nebenführ, A. A multicolored set of in vivo organelle markers for co-  
715 localization studies in Arabidopsis and other plants. *Plant J.* **51**, 1126–1136 (2007).
- 716 48. Bruno, M. & Jen, S. Cytokinin and auxin interplay in root stem-cell specification during early  
717 embryogenesis. *Nature* **4**, 1094–1097 (2008).
- 718 49. O'Malley, R. C. & Ecker, J. R. Linking genotype to phenotype using the Arabidopsis unimutant  
719 collection. *Plant J.* **61**, 928–940 (2010).
- 720 50. Park, R. J. *et al.* A genome-wide CRISPR screen identifies a restricted set of HIV host dependency  
721 factors. *Nat. Genet.* **49**, 193–203 (2017).
- 722 51. Wang, T., Wei, J. J., Sabatini, D. M. & Lander, E. S. Genetic screens in human cells using the  
723 CRISPR-Cas9 system. *Science.* **343**, 80–84 (2014).
- 724 52. Ursache, R., Fujita, S., Déneraud, V. & Geldner, N. Combined fluorescent seed selection and  
725 multiplex CRISPR/Cas9 assembly for fast generation of multiple Arabidopsis mutants. *Plant*  
726 *methods*, **17**. 111 (2021).
- 727 53. Caesar, K. *et al.* Evidence for the localization of the Arabidopsis cytokinin receptors AHK3 and  
728 AHK4 in the endoplasmic reticulum. *J. Exp. Bot.* **62**, 5571–5580 (2011).
- 729 54. Wulfetange, K. *et al.* The cytokinin receptors of arabidopsis are located mainly to the endoplasmic  
730 reticulum. *Plant Physiol.* **156**, 1808–1818 (2011).
- 731 55. Lomin, S. N., Yonekura-Sakakibara, K., Romanov, G. A. & Sakakibara, H. Ligand-binding  
732 properties and subcellular localization of maize cytokinin receptors. *J. Exp. Bot.* **62**, 5149–5159  
733 (2011).
- 734 56. Ding, W. *et al.* Isolation, characterization and transcriptome analysis of a cytokinin receptor  
735 mutant *osckt1* in rice. *Front. Plant Sci.* **8**, 1–13 (2017).
- 736 57. Antoniadi, I. *et al.* Cell-surface receptors enable perception of extracellular cytokinins. *Nat.*  
737 *Commun.* **11**, 4284 (2020).
- 738 58. Kubiasová, K. *et al.* Cytokinin fluoroprobe reveals multiple sites of cytokinin perception at plasma  
739 membrane and endoplasmic reticulum. *Nat. Commun.* **11**, 1–11 (2020).
- 740 59. Carpaneto, A. *et al.* Phloem-localized, proton-coupled sucrose carrier ZmSUT1 mediates sucrose  
741 efflux under the control of the sucrose gradient and the proton motive force. *J. Biol. Chem.* **280**,  
742 21437–21443 (2005).
- 743 60. Lérán, S. *et al.* Arabidopsis NRT1.1 is a bidirectional transporter involved in root-to-shoot Nitrate  
744 translocation. *Mol. Plant* **6**, 1984–1987 (2013).
- 745 61. Mussa Belew, Z. *et al.* Identification and characterization of phlorizin transporter from  
746 Arabidopsis 1 thaliana and its application for phlorizin production in Saccharomyces cerevisiae.  
747 *bioRxiv* (2020).
- 748 62. Chen, L. Q. *et al.* Sugar transporters for intercellular exchange and nutrition of pathogens. *Nature*  
749 **468**, 527–532 (2010).

- 750 63. Chen, J. *et al.* ABCB-mediated auxin transport in outer root tissues regulates lateral root spacing  
751 in Arabidopsis. *bioRxiv* (2020).
- 752 64. Zhang, Y. *et al.* ABA homeostasis and long-distance translocation are redundantly regulated by  
753 ABCG ABA importers. *Sci. Adv.* **7**, 1–18 (2021).
- 754 65. Develtere, W. *et al.* SMAP design: A multiplex PCR amplicon and gRNA design tool to screen for  
755 natural and CRISPR-induced genetic variation. *bioRxiv* (2022).
- 756 66. Ellison, E. E. *et al.* Multiplexed heritable gene editing using RNA viruses and mobile single guide  
757 RNAs. *Nat. Plants* **6**, 620–624 (2020).
- 758 67. Wang, M. *et al.* Gene Targeting by Homology-Directed Repair in Rice Using a Geminivirus-  
759 Based CRISPR/Cas9 System. *Mol. Plant* **10**, 1007–1010 (2017).
- 760 68. Martin-Ortigosa, S. *et al.* Mesoporous silica nanoparticle-mediated intracellular cre protein  
761 delivery for maize genome editing via loxP site excision. *Plant Physiol.* **164**, 537–547 (2014).
- 762 69. Mitter, N. *et al.* Clay nanosheets for topical delivery of RNAi for sustained protection against  
763 plant viruses. *Nat. Plants* **3**, (2017).
- 764 70. Clough, S. J. & Bent, A. F. Floral dip : a simplified method for Agrobacterium-mediated  
765 transformation of Arabidopsis thaliana. **16**, 735–743 (1999).
- 766 71. Gronau, I. & Moran, S. Optimal implementations of UPGMA and other common clustering  
767 algorithms. *Inf. Process. Lett.* **104**, 205–210 (2007).
- 768 72. Doench, J. G. *et al.* Optimized sgRNA design to maximize activity and minimize off-target effects  
769 of CRISPR-Cas9. *Nat. Biotechnol.* **34**, 184–191 (2016).
- 770 73. Li, H. & Durbin, R. Fast and accurate short read alignment with Burrows-Wheeler transform.  
771 *Bioinformatics* **25**, 1754–1760 (2009).
- 772 74. Nour-Eldin, H. H., Hansen, B. G., Nørholm, M. H. H., Jensen, J. K. & Halkier, B. A. Advancing  
773 uracil-excision based cloning towards an ideal technique for cloning PCR fragments. *Nucleic  
774 Acids Res.* **34**, (2006).
- 775 75. Jørgensen, M., Crocoll, C., Halkier, B. & Nour-Eldin, H. Uptake Assays in *Xenopus laevis*  
776 Oocytes Using Liquid Chromatography-mass Spectrometry to Detect Transport Activity. *Bio-  
777 Protocol* **7**, 1–13 (2017).
- 778 76. Ionescu, I. A. *et al.* Transcriptome and metabolite changes during hydrogen cyanamide-induced  
779 floral bud break in sweet cherry. *Front. Plant Sci.* **8**, 1–17 (2017).
- 780 77. Jarzyniak, K. *et al.* Early stages of legume–rhizobia symbiosis are controlled by ABCG-mediated  
781 transport of active cytokinins. *Nat. Plants* **7**, (2021).
- 782 78. Dereeper, A. *et al.* Phylogeny.fr: robust phylogenetic analysis for the non-specialist. *Nucleic Acids  
783 Res.* **36**, 465–469 (2008).
- 784 79. Prasad, K. *et al.* Arabidopsis PLETHORA transcription factors control phyllotaxis. *Curr. Biol.* **21**,  
785 1123–1128 (2011).
- 786
- 787



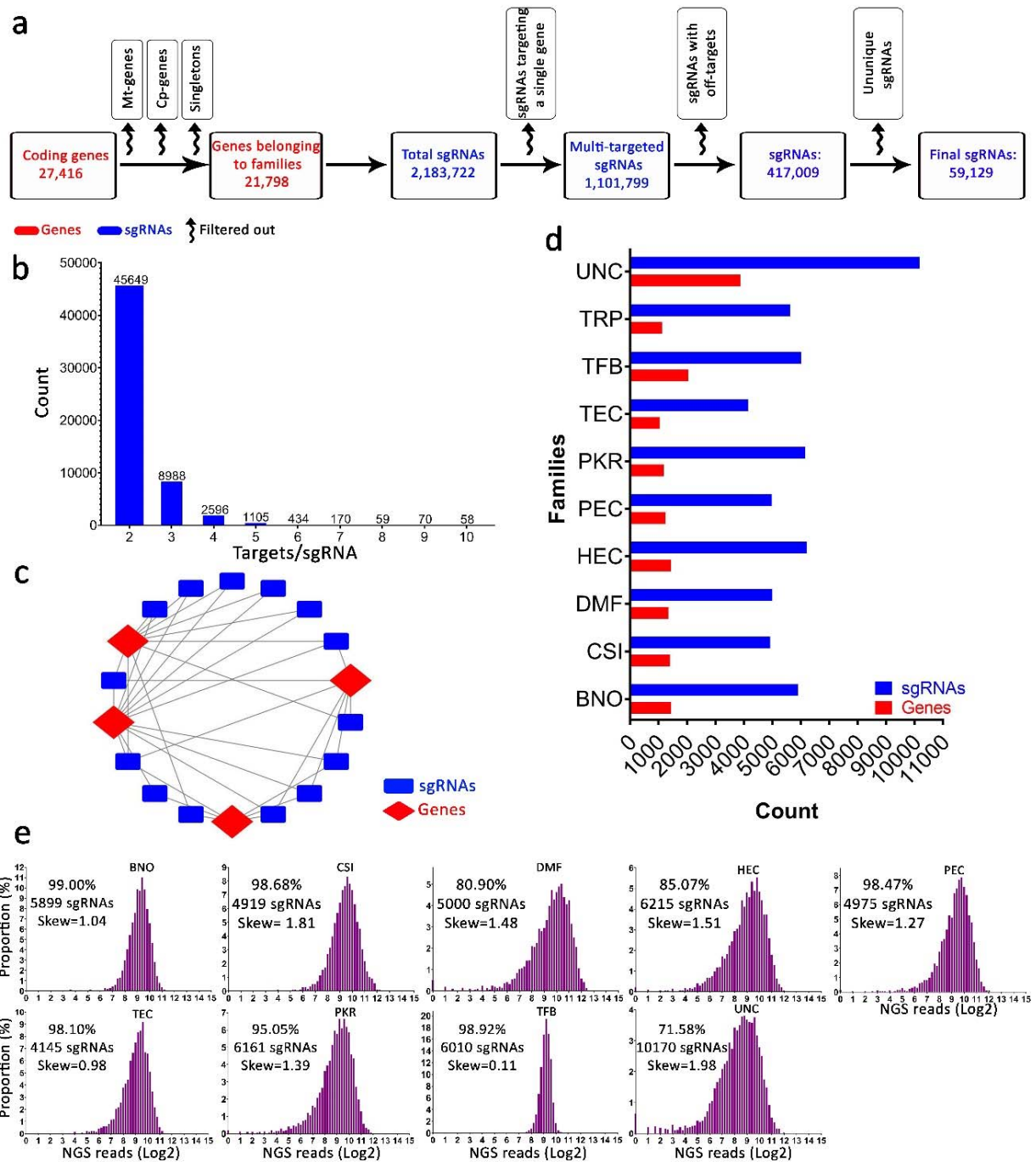
788

789 **Fig. 1: Overview of the Multi-Knock, genome-scale, multi-targeted CRISPR platform.** Stage 1: Multi-  
 790 targeted sgRNAs were designed to target multiple genes (coding sequences) from the same family. The  
 791 *Arabidopsis* genome was clustered into gene families and multiple sgRNAs were designed to target each node  
 792 using the CRISPys algorithm. Stages 2 and 3: sgRNA sub-library sequences were synthesized, amplified, and  
 793 cloned into CRISPR/Cas9 vectors. Stage 4: The pooled CRISPR library was introduced into *Agrobacterium* and  
 794 transformed into *Arabidopsis* to generate stable lines. Each plant expresses a single sgRNA, targeting a clade of 2  
 795 to 10 genes from the same family. Stage 5: A phenotypic forward genetic screen was conducted. Candidate lines  
 796 were genotyped for sgRNAs and targets.  
 797



798

799 **Fig. 2: An overview of sgRNA design strategy for gene families.** **a**, For each gene family, the multiple  
 800 alignments of the respective protein sequences is computed.  $P$  stands for protein, and letters indicate amino  
 801 acids. **b**, A phylogenetic tree is constructed based on the sequence similarity of the protein sequences.  
 802 Optimal sgRNAs for each subgroup of genes, which are induced by internal nodes in the tree (marked by  
 803 lowercase letters  $a$ - $c$ ), are then designed. **c**, For each subfamily of genes, and illustrated here for node  $a$ , all  
 804 potential CRISPR target sites are extracted. In this case, the subfamily induced by node  $a$  includes two  
 805 genes ( $g_2$  and  $g_4$ , encoding for proteins  $P_2$  and  $P_4$ , respectively). Typically, each gene contains dozens of  
 806 possible targets. For simplicity, only five targets are presented. Nucleotide positions that are identical in all  
 807 targets are colored in black, while the polymorphic sites are colored in red and are in bold type. **d**, A tree  
 808 of the target sites is constructed based on sequence similarity among the targets while accounting for  
 809 CRISPR-specific characteristics. sgRNA candidates are constructed for each internal node, where all  
 810 combinations of the polymorphic sites are considered (marked in red), and the ones with the highest editing  
 811 efficacy to target the considered subgroup of genes are chosen. For simplicity, only a few candidates  
 812 (denoted by  $s_i$ ) are shown for each internal node. Assuming that the cutoff of the number of polymorphic  
 813 sites  $k$  is 4, the search of sgRNA candidates stops at node  $z$ . In practice,  $k$  was set to 12 polymorphic sites.

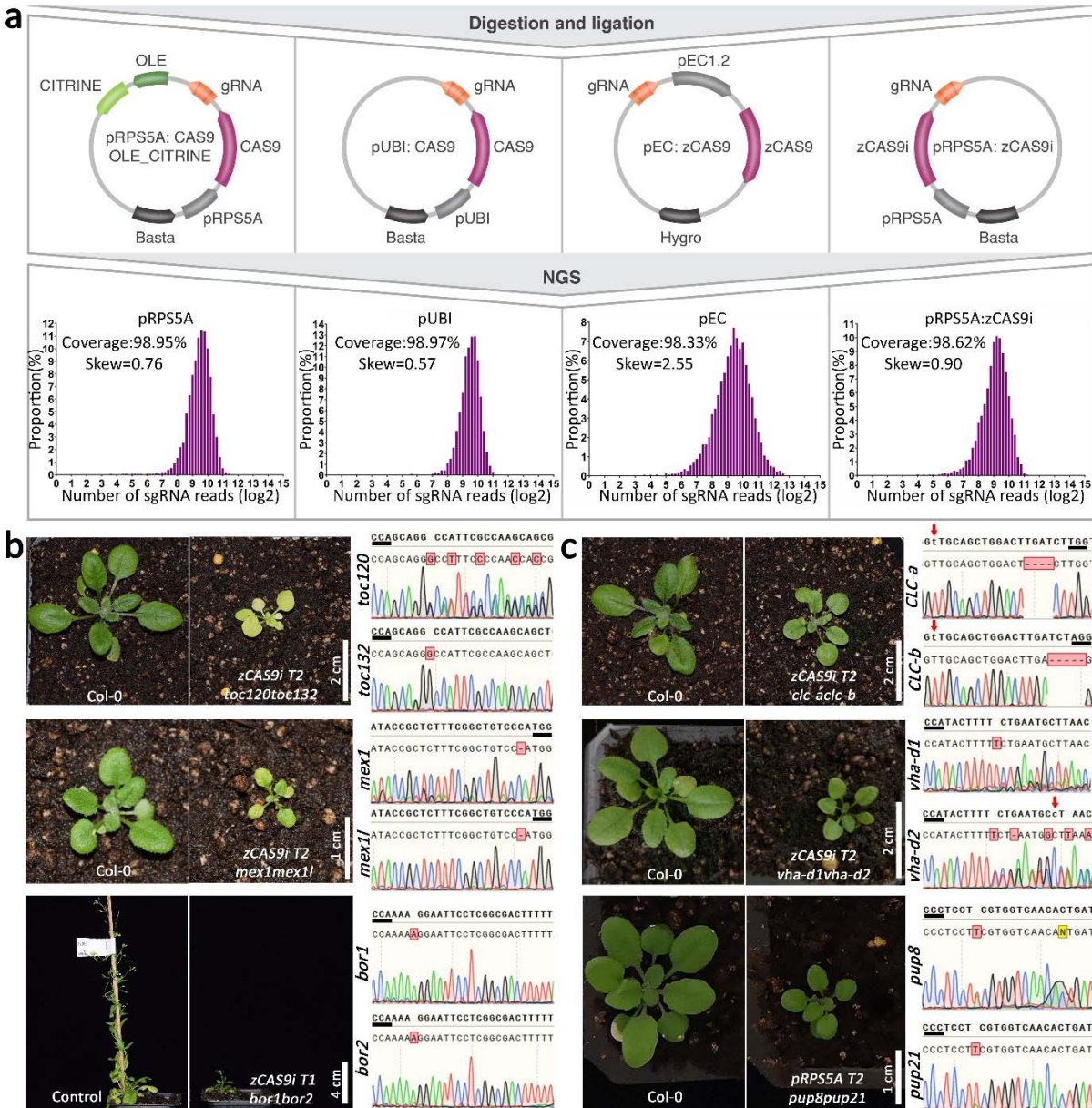


814

815 **Fig. 3: Multi-targeted genome-scale sgRNA design and construction.** **a**, Schematic illustration of the  
 816 computational workflow used to design the Multi-Knock sgRNA library. A filtering process yielded a selection  
 817 of 59,129 sgRNAs targeting 16,152 genes (~74% of all coding genes belonging to families). The red color  
 818 represents coding genes, blue color represents sgRNAs, and curved arrows represent filtering steps. Abbreviations:  
 819 Mt-genes, mitochondrial genes; Cp-genes, chloroplast genes; Singletons, genes that do not belong to a family. **b**,  
 820 Histogram showing the number of genes targeted by individual sgRNAs. **c**, Representative sgRNA-target network  
 821 in the CRISPR library. Genes are targeted by multiple sgRNAs, and sgRNAs target multiple genes. **d**, Total number  
 822 of sgRNAs and target genes in each functional sub-library. **e**, Deep-sequencing data of sgRNAs in individual sub-  
 823 libraries. Columns indicate the distribution of sgRNAs. Coverage is indicated for each group. TRP (transporters);

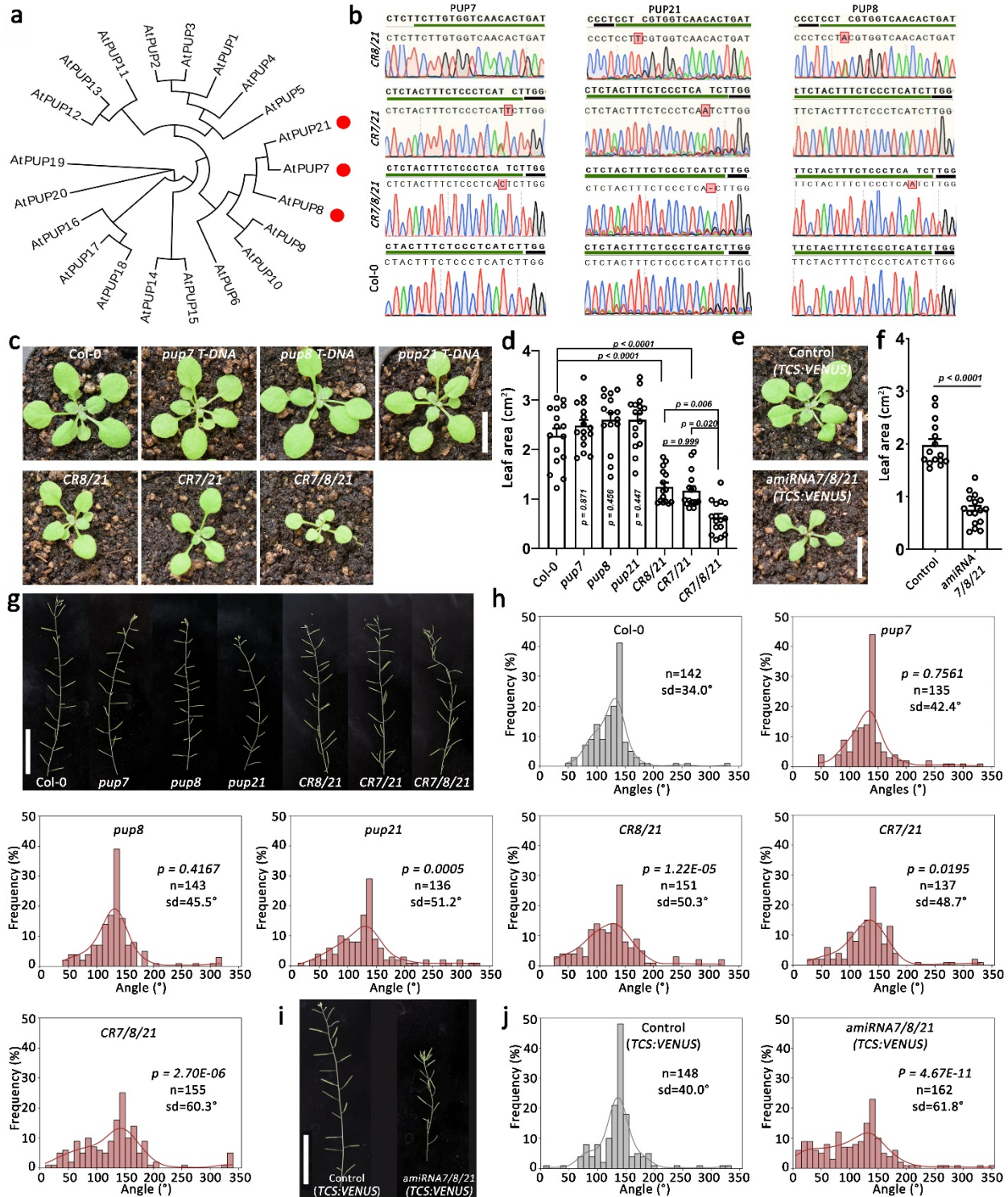
824 PKR (protein kinases, protein phosphatases, receptors, and their ligands); TFB (transcription factors and  
825 other RNA and DNA binding proteins); BNO (proteins binding small molecules); CSI (proteins that form  
826 or interact with protein complexes including stabilizing factors); HEC (hydrolytic enzymes); TEC  
827 (metabolic enzymes and enzymes that catalyze transfer reactions); PEC (catalytically active proteins,  
828 mainly enzymes); DMF (proteins with diverse functional annotations not found in the other categories);  
829 and UNC (proteins of unknown function or cannot be inferred).  
830





831

832 **Fig. 4: Transportome-specific Multi-Knock screen.** **a**, To create independent sub-libraries, 5,635 sgRNAs, each  
 833 targeting 2 to 10 transporters from the same family, were amplified and cloned into four different Cas9 vectors to  
 834 create pRPS5A:Cas9 (OLE:CITRINE), pUBI:Cas9, pEC:Cas9, and pRPS5A:zCas9i sub-libraries. Graphs show  
 835 coverage and frequency based on next-generation sequencing of the four sub-libraries. The four libraries were  
 836 transformed into Col-0 plants yielding 3,500 transgenic T1 plants. **b**, Photographs show representative phenotypes  
 837 of TRP Multi-Knock proof-of-concept lines. From top to bottom are Col-0 and plant expressing sgRNA targeting  
 838 *toc120* and *toc132* (scale bar = 2 cm), Col-0 and plant expressing sgRNA targeting *mex1* and *mex11* (scale bar = 1  
 839 cm), and control *DR5:VENUS* plant and the T1 plant harboring sgRNA targeting *bor1* and *bor2* (scale bar = 4 cm).  
 840 Chromatograms show the types of mutations. Red arrows indicate the mismatches between sgRNA and target  
 841 sequence. PAM is marked with a black underline. **c**, Images show lines with abnormal phenotypes that had not  
 842 previously been described: from top to bottom adjacent to Col-0 control are plants expressing sgRNA targeting *clc-*  
 843 *a* and *clc-b* (scale bar = 2 cm), *vha-d1* and *vha-d2* (scale bar = 2 cm), and *pup8* and *pup21* (scale bar = 1 cm).  
 844 Chromatograms show the type of mutations. Red arrows indicate the mismatches between sgRNA and target  
 845 sequence. PAM is marked with a black underline.



846  
847

848 **Fig. 5: PUP7, 8, and 21 redundantly regulate shoot growth and phyllotaxis.** **a**, Phylogenetic tree of *Arabidopsis*  
 849 PUP family based on amino acid sequences. Red dots indicate proteins coded by putative *CR7/8/21* target genes.  
 850 **b**, Chromatograms showing the types of mutations in the *CR8/21* (T3 generation), *CR7/21* (T3 generation) and  
 851 *CR7/8/21* (T4 generation) lines as identified by sequencing. *CR8/21* and *CR7/21* stand for CRISPR double mutant  
 852 *pup8/21* and *pup7/21*, respectively; *CR7/8/21* stands for CRISPR triple mutant *pup7/8/21*. PAM is underlined in

853 black; 20-bp sgRNA is underlined in green. The sgRNA in line *CR8/21* was not designed to target PUP7 as it does  
854 not contain a respective PAM sequence. **c**, Shown are representative images of 18-day-old WT (Col-0), the T-  
855 DNA single *pup7*, *pup8*, *pup21* mutants, the double *pup8pup21* (*CR8/21*) (T3 generation), double  
856 *pup7pup21* (*CR7/21*) (T3 generation), and the triple *pup7pup8pup21* CRISPR mutant (*CR7/8/21*) (T4  
857 generation). Scale bar = 1 cm. **d**, Quantification of genotypes shown in (c). Shown are means ( $\pm$ SE). *p* value  
858 in ordinary one-way ANOVA is indicated for each analysis. Col-0, *pup7*, *pup21*, *CR7/21* and *CR7/8/21*:  
859 *n*=16; *pup8* and *CR8/21*: *n*=15. **e**, Shown are representative images of 18-day-old Control (*TCS:VENUS*)  
860 and *amiRNA7/8/21* (*TCS:VENUS* background). *amiRNA7/8/21* stands for amiRNA knockdown *PUP7/8/21*.  
861 Scale bar = 1 cm. **f**, Quantification of genotypes shown in (e). Shown are means ( $\pm$ SE). *p* value two tailed  
862 *t* test is indicated. *n* = 15 (Control); *n* = 16 (*amiRNA7/8/21*). **g**, Phyllotaxis patterns in inflorescences stem of  
863 wild-type (Col-0), single T-DNA insertion mutants, *CR8/21*, *CR7/21* and *CR7/8/21*. Scale bar = 5 cm. **h**, Silique  
864 divergence angle distribution in inflorescences of Col-0, *pup* single mutants, *CR8/21*, *CR7/21* and *CR7/8/21*. *P*-  
865 value, *n* number and standard deviation (sd) are indicated for each analysis. *P*-value was extracted using Fligner-  
866 Killeen test for equality of variance. **i**, Phyllotaxis patterns in inflorescence stem of control (*TCS:VENUS*) and  
867 *amiRNA7/8/21* mutant. *amiRNA7/8/21* stands for amiRNA triple *PUP7/8/21* knockdown. Scale bar = 5 cm. **j**,  
868 Distribution of divergence angle frequencies between successive siliques in control and *amiRNA7/8/21* stems. *p*  
869 value Fligner-Killeen test for equality of variance is indicated for each analysis.

870

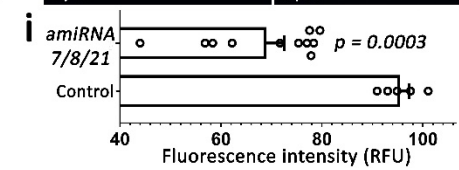
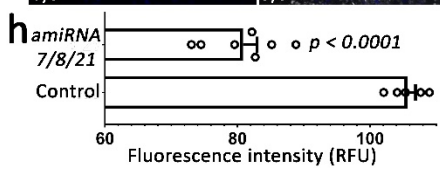
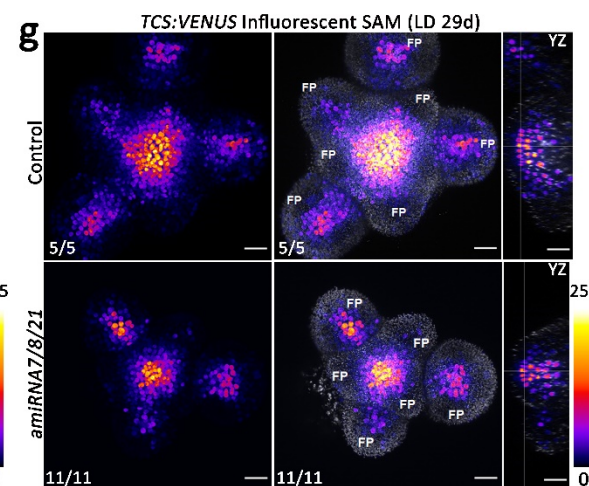
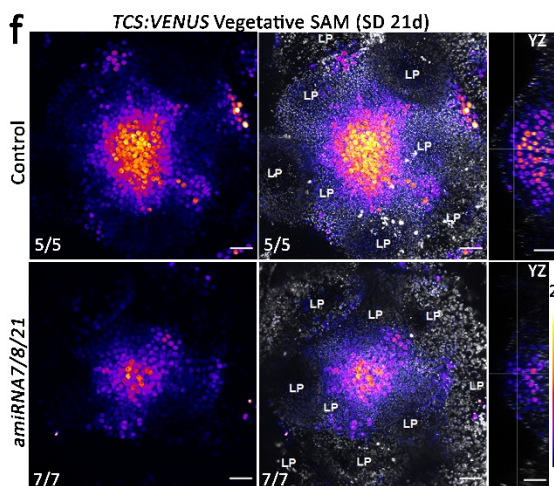
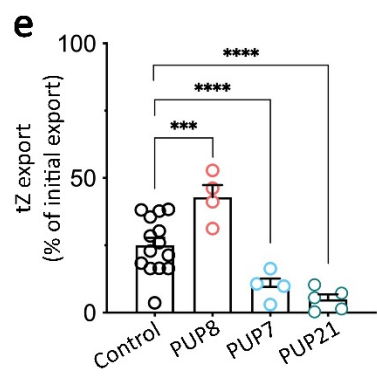
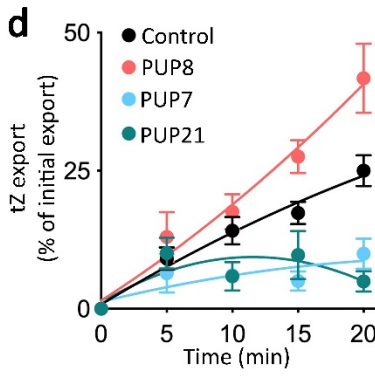
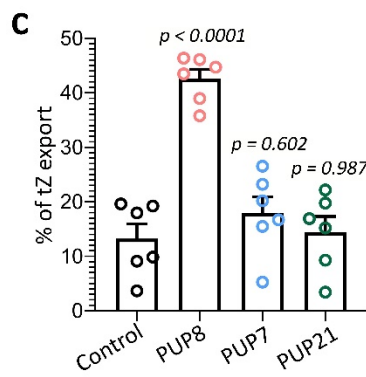
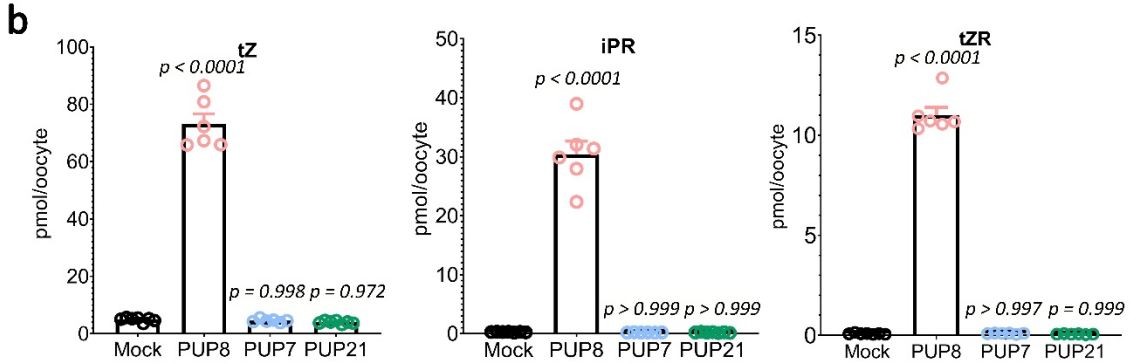
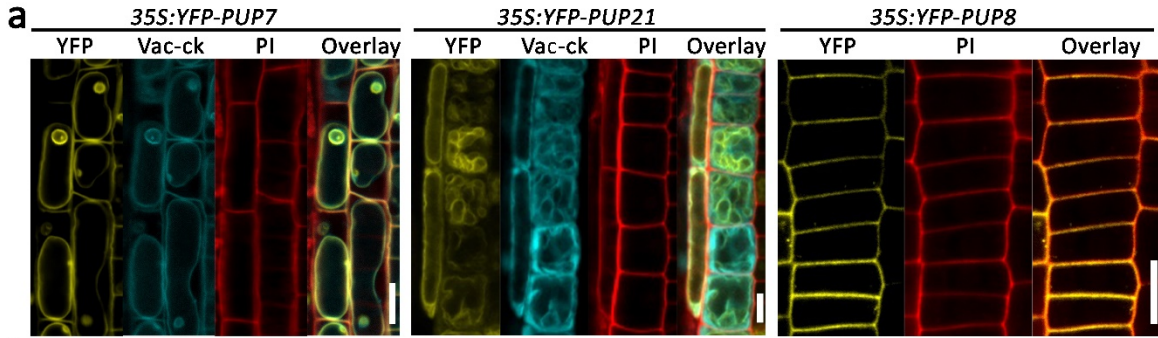
871

872

873

874





876 **Fig. 6: PUP7, PUP8, and PUP21 regulate cytokinin transport and shoot meristem.** **a**, Root meristem confocal  
877 microscopy images of *35S:YFP-PUPs* localization. YFP (yellow) was used to label PUPs, Vac-ck (cyan) was used  
878 as a tonoplast marker, and propidium iodide (PI) (red) was used to stain the cell wall. Scale bars = 10  $\mu$ m. **b**,  
879 Standard import *Xenopus laevis* oocytes assays using the indicated cytokinin froms. 60 min transport assay  
880 in 100  $\mu$ M cytokinins at pH = 5.5. n = 6-7, shown are means ( $\pm$ SE). *p* value two tailed *t* test is indicated for  
881 each analysis. **c**, Injection-based export assay of PUPs in *Xenopus laevis* oocytes. n = 6  $\pm$  SE, *p* value two-tailed  
882 *t*-test is indicated for each analysis. **d, e**, tZ export from tobacco protoplasts as percentage of initial export as a  
883 function of time (**d**) and at 20 minutes (**e**). n  $\geq$  4, \*\*\* *p* < 0.001, \*\*\*\* *p* < 0.0001; One-way ANOVA. **f-i**,  
884 *TCS-Venus* intensity in control plants (*TCS:VENUS*) compared to *amiR7/8/21* at (**f**) vegetative and (**g**)  
885 inflorescence stages. *amiRNA7/8/21* stands for amiRNA triple knockdown *PUP7/8/21*. Optical longitudinal  
886 sections of the meristem (YZ direction) are shown. Scale bars = 100  $\mu$ m. The color scale at the right indicates *TCS*  
887 expression. Quantification of *TCS-Venus* intensity in vegetative (**h**) and inflorescence (**i**) stages. Control: n = 5 in  
888 (**h, i**); *amiRNA7/8/21*: n = 7 in (**h**), n = 11 in (**i**). Shown are means ( $\pm$ SE). *p* value two tailed *t* test is indicated for  
889 each analysis.  
890

# Supplemental Data

## **Multi-Knock – a multi-targeted genome-scale CRISPR toolbox to overcome functional redundancy in plants**

Yangjie Hu<sup>1</sup>, Priyanka Patra<sup>1,2,\*</sup>, Odelia Pisanty<sup>1,\*</sup>, Anat Shafir<sup>1</sup>, Zeinu Mussa Belew<sup>3</sup>, Jenia Binenbaum<sup>1</sup>, Shir Ben Yaakov<sup>1</sup>, Bihai Shi<sup>2</sup>, Laurence Charrier<sup>4</sup>, Gal Hyams<sup>1</sup>, Yuqin Zhang<sup>1</sup>, Maor Trabolsky<sup>1</sup>, Omer Caldararu<sup>1</sup>, Daniela Weiss<sup>1</sup>, Christoph Crocoll<sup>3</sup>, Adi Avni<sup>1</sup>, Teva Vernoux<sup>2</sup>, Markus Geisler<sup>4</sup>, Hussam Hassan Nour-Eldin<sup>3</sup>, Itay Mayrose<sup>1,✉</sup>, and Eilon Shani<sup>1,✉</sup>

<sup>1</sup> School of Plant Sciences and Food Security, Tel Aviv University, Tel Aviv, 69978, Israel

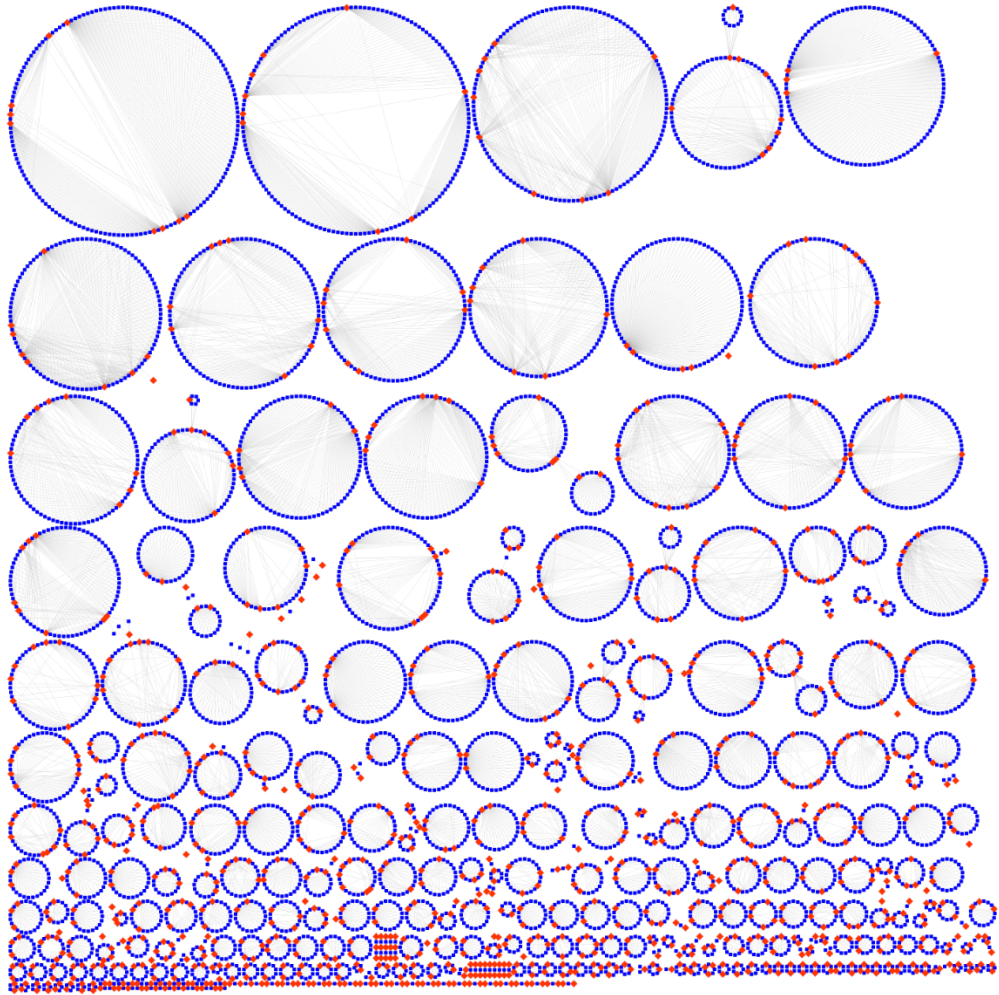
<sup>2</sup> Laboratoire Reproduction et Développement des Plantes, Université de Lyon, ENS de Lyon, UCB Lyon 1, CNRS, INRAE, INRIA, Lyon, France

<sup>3</sup> DynaMo Center, Department of Plant and Environmental Sciences, University of Copenhagen, Frederiksberg, 1871, Denmark

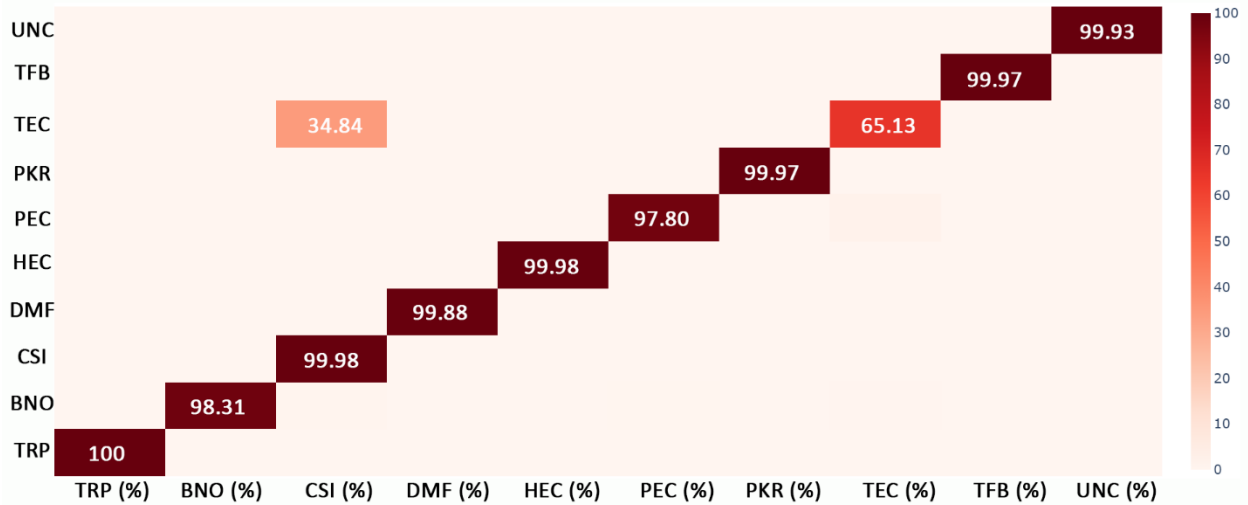
<sup>4</sup> Department of Biology, University of Fribourg, CH-1700 Fribourg, Switzerland

\* Equal contribution

✉ Corresponding author

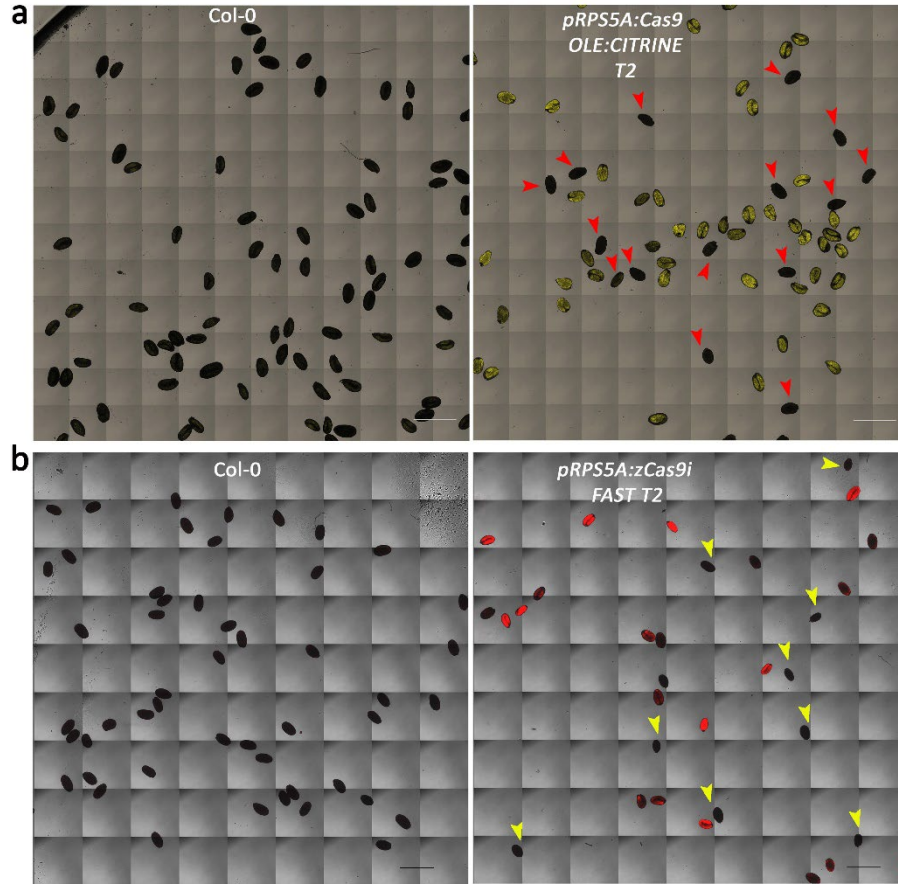


**Supplementary Figure 1: Transportome Multi-Knock network.** Overview of sgRNAs (blue) and the targeted genes (red) network for the CRISPR library targeting the transporters family. Shown are 1,123 transporter genes (red) and 5,635 sgRNAs (blue).

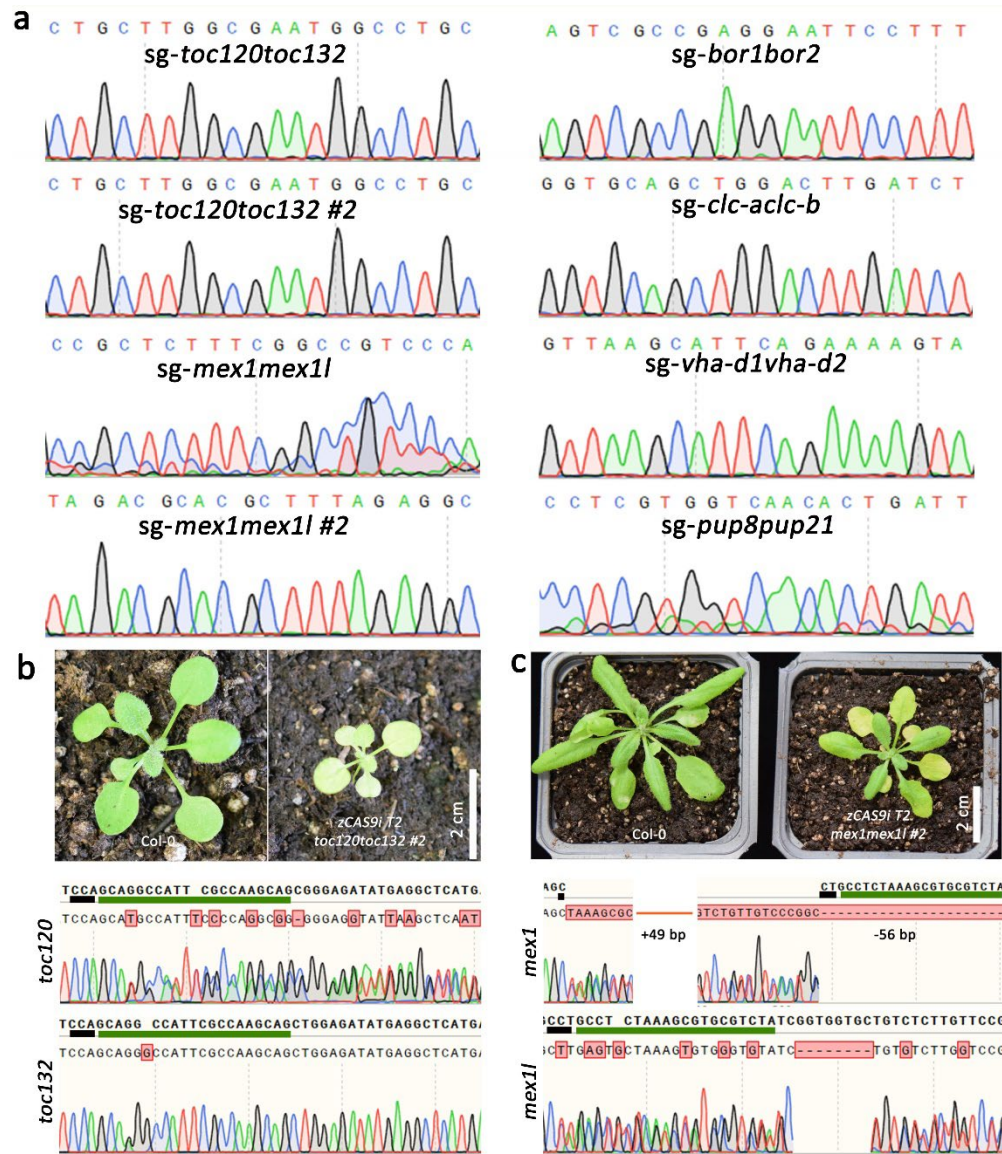


**Supplementary Figure 2: sgRNAs cross-contamination analysis of the ten sub-libraries based on next-generation sequencing.** Heatmap illustrating the percentage of sgRNAs for each individual sub-library. The color scale bar reflects the relative percentage. All libraries are highly specific, except for TEC which shows significant amplification of the CSI sub-library. TRP (transporters); PKR (protein kinases, protein phosphatases, receptors, and their ligands); TFB (transcription factors and other RNA and DNA binding proteins); BNO (proteins binding small molecules); CSI (proteins that form or interact with protein complexes including stabilizing factors); HEC (hydrolytic enzymes); TEC (metabolic enzymes and enzymes that catalyze transfer reactions); PEC (catalytically active proteins, mainly enzymes); DMF (proteins with diverse functional annotations not found in the other categories); and UNC (proteins of unknown function or cannot be inferred).

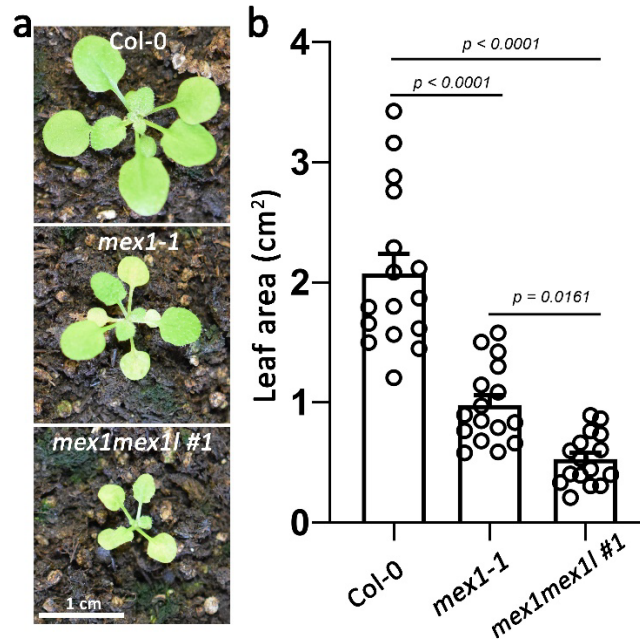




**Supplementary Figure 3. Visual fluorescence segregation for Cas9-free seeds.** **a**, Cas9-free seeds selection in pRPS5A:Cas9 OLE:CITRINE T2 seeds. Yellow signal in seeds indicates for OLE:CITRINE. The Cas9-free seeds, which do not produce the yellow fluorescence, are marked by red arrows. Scale bar = 1 mm. **b**, Cas9-free seeds selection in pRPS5A:zCas9i *FAST* T2 seeds. The Cas9-free seeds, which do not produce the red fluorescence, are marked by yellow arrows. *FAST* (pOLE1:tagRFP)<sup>1</sup>. Scale bar = 1 mm.

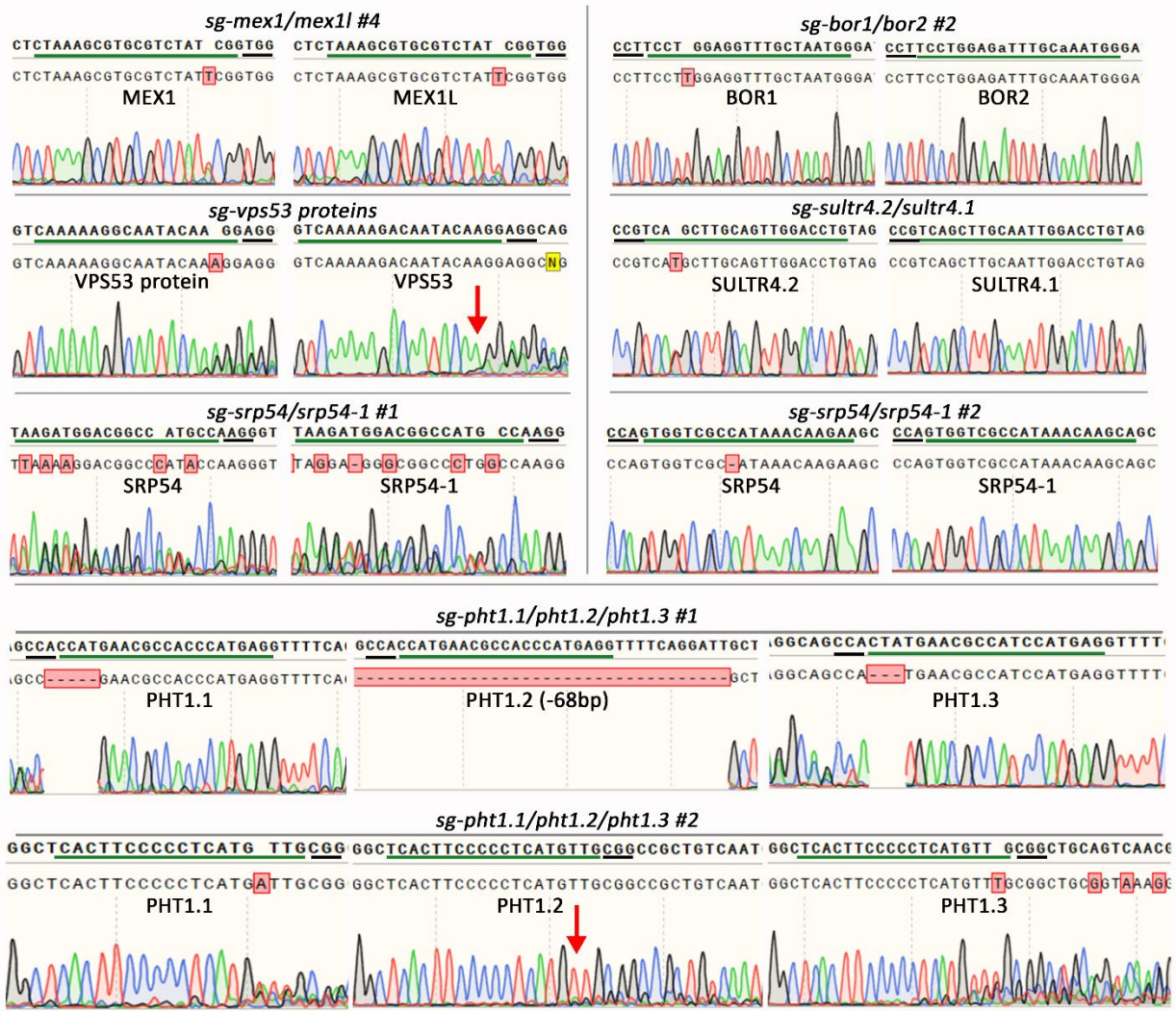


**Supplementary Figure 4. Sequencing data for multiple sgRNA and their putative target genes. a,** Chromatograms show sgRNA sequences of the indicated TRP Multi-Knock lines. Lines are presented in Fig 4. Two additional lines are presented for *toc132toc120* and *mex1mex1l* (#2). **b,c,** Shown are *toc132toc120* (**b**) and *mex1mex1l* (**c**) knockout alleles, which are additional to the lines presented in Fig 4. Photographs show an independent line for *toc120toc132* #2 (left). Chromatograms indicate for the types of mutation (left). Images show a similar independent line for *mex1mex1l* #2 (right). Chromatograms indicate for the types of mutation (right). Scale bar = 2 cm; PAM is marked with a black underline; 20-bp gRNA is underlined in green.

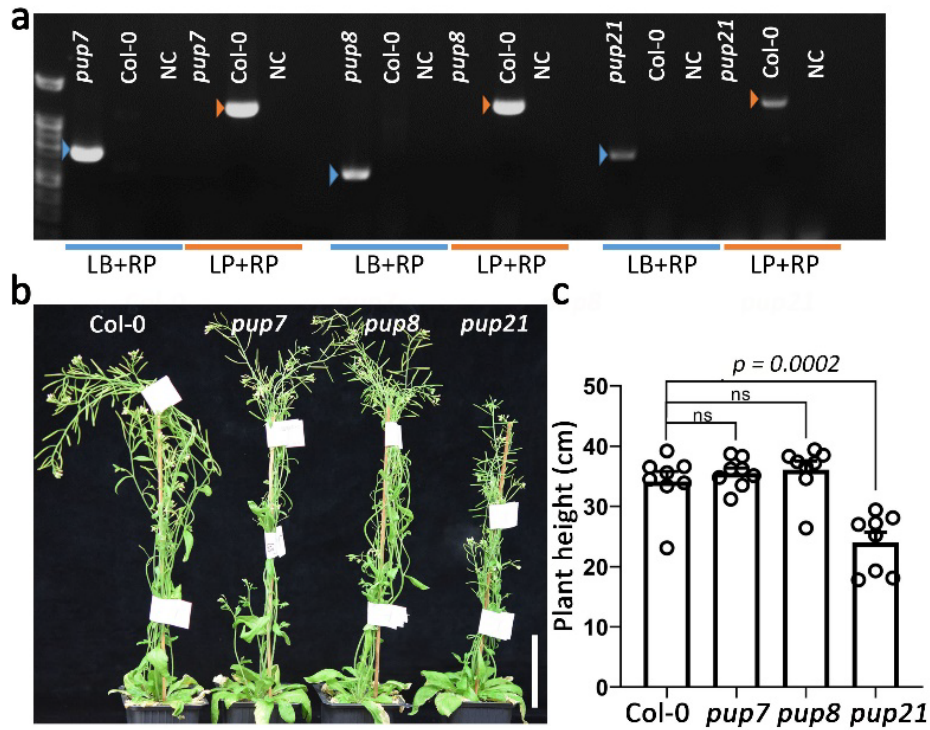


**Supplementary Figure 5. *mex1* and *mex11*, single and double knockout phenotypes. a,** Representative images showing shoot phenotypes of 18-day-old of the wild type (Col-0), single (*mex1-1*) and double mutant homozygous plants (*mex1mex11 T3 #1*). Scale bar = 1 cm. **b,** Quantification of phenotypes shown in (a). Shown are means ( $\pm$ SE),  $n = 16$  plants,  $p$  value two tailed  $t$ -test is indicated.

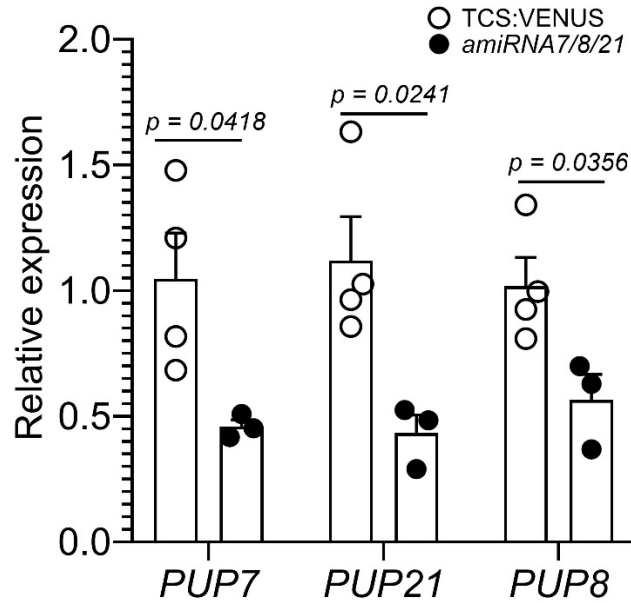




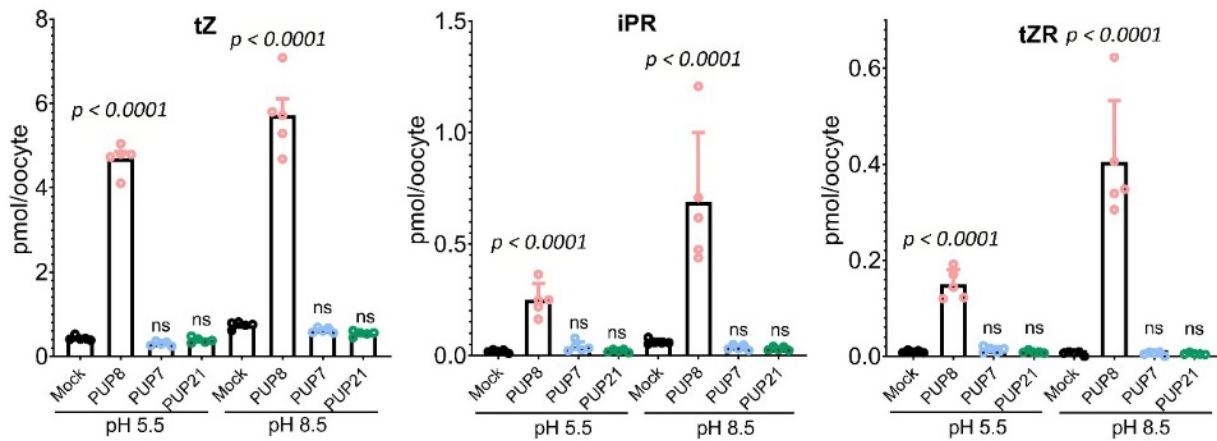
**Supplementary Figure 6. Single, double, and triple mutants generated by Multi-Knock.** Shown are Sanger sequencing chromatograms indicating the type of mutation in T2 lines. *mex1mex1l #4* and *bor1bor2 #2* are additional lines (independent lines) to the ones presented in Fig. 4 and Sup. Fig. 4. Two similar independent lines with different sgRNAs targeting the same targets (Phosphate transporters: PHT1.1, PHT1.2, and PHT1.3) show different mutation types. The ambiguous peak is indicated by a red arrow. PAM is marked with a black underline; 20-bp gRNA is underlined in green.



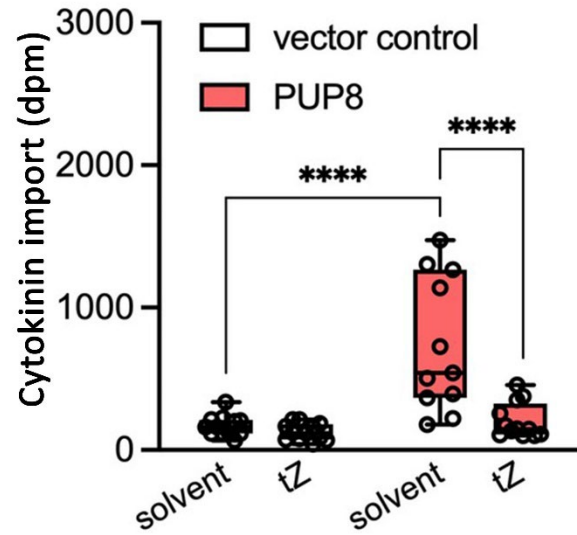
**Supplementary Figure 7: Characterization of single T-DNA insertion mutants.** **a**, Genotyping of the *pup7*, *pup8*, *pup21* single mutant plants compared to Col-0. Orange arrows indicate for WT amplification bands, blue arrows indicated for T-DNA insertion amplification bands. LB: left border primer of T-DNA insertion, LP: left genomic primer, RP: right genomic primer, NC: negative control. **b**, Plant height of 58-day-old plants of the indicated genotypes. **c**, Quantification of plant height. Shown are means ( $\pm$ SE),  $n = 8$  plants,  $p$  value two tailed  $t$ -test is indicated. Scale bar = 5 cm



**Supplementary Figure 8: PUP7, PUP8, and PUP21 are down-regulated in *amiR7/8/21*.** Relative expression of the indicated PUP *amiR7/8/21*-targeted genes in 15-day-old seedlings, quantified by qRT-PCR. *amiRNA7/8/21* stands for amiRNA triple knockdown PUP7/8/21. Shown are averages ( $\pm$ SE),  $n = 4$  (Control),  $n = 3$  (*amiR7/8/21*);  $p$  value two tailed  $t$  test is indicated for each analysis.



**Supplementary Figure 9: PUP8 promotes cytokinin uptake in *Xenopus laevis* oocytes.** 60 min transport assay in 10  $\mu$ M cytokinin at pH = 5.5 and pH = 8.5.  $n = 5 \pm$ SE,  $p$  value two tailed  $t$ -test is indicated for each analysis.



**Supplementary Figure 10: PUP8 tZ competition assays.**  $^3\text{H}$ -tZ import into microsomal fractions prepared from tobacco leaves infiltrated with vector control and 35S:YFP-PUP8 (PUP8), conducted in the absence (solvent) and presence of a 1,000-fold excess of non-labelled tZ. Significant differences of means to solvent control were determined by ordinary One-way ANOVA; \*\*\*  $p < 0.001$ , \*\*\*\*  $p < 0.0001$  ( $n \geq 4$ ).

**Supplementary Table 1. Overview of sgRNAs and gene numbers per family.**

<b>Families</b>	<b>Targeted genes per family (Coverage %)</b>	<b>Genes per family</b>	<b>sgRNAs per family</b>
<b>BNO</b>	1443 (76.1%)	1896	5899
<b>CSI</b>	1399 (82.7%)	1692	4919
<b>DMF</b>	1343 (71.0%)	1891	5000
<b>HEC</b>	1438 (84.3%)	1706	6215
<b>PEC</b>	1252 (82.6%)	1515	4975
<b>PKR</b>	1190 (84.7%)	1405	6161
<b>TEC</b>	1041 (86.0%)	1211	4145
<b>TFB</b>	2042 (78.2%)	2611	6010
<b>TRP</b>	1123 (84.6%)	1327	5635
<b>UNC</b>	3881 (59.3%)	6544	10170



**Supplementary Table 2. Adaptor sequences for each Multi-Knock group.**

Adaptor sequences are marked in blue.

Pools	Pool description	Adaptor sequence + sgRNA
<b>PKR</b>	Protein kinases, protein phosphatases, receptors, and their ligands	CTGGTCATCATCCTGCCTTggtctcGattgNNNNNNNNNNNNNNNNNNNN GTTTcGAGACCTGTTATATGGAGGGGGCAA (82 bp)
<b>BNO</b>	Protein binding small molecules	GGATTATTCATACCGTCCC AggtctcGattgNNNNNNNNNNNNNNNNNNNN GTTTcGAGACCAATCAGCCATACCACATTG (82 bp)
<b>CSI</b>	Proteins that form or interact with protein complexes including stabilization of those	AGAGCTCGTTTGTAGTGAACCGggtctcGattgNNNNNNNNNNNNNNNNNNNN GTTTcGAGACCGATGAGTTTGGACAAACCAC (82 bp)
<b>TFB</b>	Transcription factors	CGTTGGCTACCCGTGATTTggtctcGattgNNNNNNNNNNNNNNNNNNNN GTTTcGAGACCCTATTCCGGCTATGACTGGGC (82 bp)
<b>TEC</b>	Metabolic and other enzymes catalyzing transfer reactions	TGTA AACGACG GCCAGTggtctcGattgNNNNNNNNNNNNNNNNNNNN GTTTcGAGACCCTGAATCATGGTCATAGCTGTT (82bp)
<b>PEC</b>	Active catalytic proteins, mainly enzymes	GAAACAGCTATGACCATGggtctcGattgNNNNNNNNNNNNNNNNNNNN GTTTcGAGACCGTCGTGACTGGGAAAACC (79 bp)
<b>UNC</b>	Genes for which the function is not known or cannot be inferred	CGACTCACTATAGGGAGAGCGGCggtctcGattgNNNNNNNNNNNNNNNNNNNN GTTTcGAGACCCTGCCATGGAAAATCGATGTTCTT (89 bp)
<b>DMF</b>	A protein with diverse functional annotation not found in the other categories	TCCTCCGTTATTGATATGCGggtctcGattgNNNNNNNNNNNNNNNNNNNN GTTTcGAGACCCTGTACTGACTTTTACTCC (84 bp)
<b>HEC</b>	Hydrolytic enzymes, excluding protein phosphatases	GCGAGAGTAGGGAACTGCggtctcGattgNNNNNNNNNNNNNNNNNNNN GTTTcGAGACCGTGTCTCAAATCTCTGATGTT (82 bp)
<b>TRP</b>	Transporters	CCAAGCTATTTAGGTGACACggtctcGattgNNNNNNNNNNNNNNNNNNNN GTTTcGAGACC TAGAAGGCACAGTCGAGG (80 bp)

Adaptor sequence      *Bsal*    sgRNA (20 bp)    *Bsal*    Adaptor sequence

TGTA AACGACG GCCAGTGGTCTCGattgNNNNNNNNNNNNNNNNNNNNgttcGAGACCGTAATCATGGTCATAGCTGTT

**Example of the sgRNAs Multi-Knock oligonucleotides design.** The 20-bp sgRNA is shown in red letters and two *Bsal* sites are marked by purple rectangles. Adaptors are shown in blue.

**Supplementary Table 3. Primers for amplification of subgroups of sgRNA library**

<b>Pools</b>	<b>Forward primer (5'-3')</b>	<b>Reverse primer (5'-3')</b>
<b>PKR</b>	CTGGTCATCATCCTGCCTTT	TTTGCCCCCTCCATATAACA
<b>BNO</b>	GGATTATTCATACCGTCCCA	CAAATGTGGTATGGCTGATT
<b>CSI</b>	AGAGCTCGTTTAGTGAACCG	GTGGTTTGTCCAAACTCATC
<b>TFB</b>	CGTTGGCTACCCGTGATATT	GCCCAGTCATAGCCGAATAG
<b>TEC</b>	TGTAAAACGACGGCCAGT	AACAGCTATGACCATGATTACG
<b>PEC</b>	GGAAACAGCTATGACCATG	GGTTTTCCAGTCACGAC
<b>UNC</b>	CGACTCACTATAGGGAGAGCGGC	AAGAACATCGATTTTCCATGGCAG
<b>DMF</b>	TCCTCCGCTTATTGATATGC	GGAAGTAAAAGTCGTAACAAGG
<b>HEC</b>	GCGAGAGTAGGGAAGTGC	AACATCAGAGATTTTGAGACAC
<b>TRP</b>	CCAAGCTATTTAGGTGACACGG	CCTCGACTGTGCCTTCTAGG

**Supplementary Table 4. Primers for NGS PCR amplification and sgRNAs genotyping in transgenic plants.**

<b>Cas9 expression constructs</b>	<b>Forward primer (5'-3')</b>	<b>Reverse primer (5'-3')</b>
pRPS5A:zCas9i	TACTAGATCGACGCTACTAG	CCGACTCGGTGCCACTTTT
pUBI:Cas9	CCCCTGGGAATCTGAAAGAAG	CCGACTCGGTGCCACTTTT
pEC:Cas9	CCCCTGGGAATCTGAAAGAAG	CCGACTCGGTGCCACTTTT
pRPS5A:Cas9 OLE:CITRIN	CCCCTGGGAATCTGAAAGAAG	CCGACTCGGTGCCACTTTT

**Supplementary Table 5. Primers used for PCR-based genotyping.**

<b>Targets</b>	<b>Forward primer (5'-3')</b>	<b>Reverse primer (5'-3')</b>
TOC120	CTCTTACGCACCATCACTG	GCTTCGGCAAGAATCTTGG
TOC132	TCTCCTGCGCACCATAAGT	TCACCATACTGCTGTTTCAG
MEX1	AGGGAAATCCAGGTTTGGG	CTGCCACAGCAATACCAAAG
MEX1L	AGGGAAATCCAGGTTTGGG	GAGTAGAGACCACTCCAG
BOR1	GCTTTTCATGCAGCAAGCCA	GAACATCAAGCATCTCCTGC
BOR2	GGCCTTCTTATAGCTATGCTC	GGAAGTTGAAGCATCTCCTGA
CLC-a	GACACTCCCAATATGTTTGG	CAGAGGCAGATCCACATGT
CLC-b	GGAATCCCTGAGATCAAAGC	AGTACACCTCCAACAGGTG
VHA-d1	CCGCATCAACCTTTTCCATC	GAGGGTGTTCCTCATAATCTC
VHA-d2	CCCTTAGCTGTTTCATAACCC	CAAGGTATGCTTTGTAGAGGG
PUP7	CTCTTTTGCCAGCCACTAGCT	CCACAAGAAGAGCAGAGGATACAG
PUP8	CCCAAACCAAAAATCCCAAACC	CCAGGGATAGCAGCAATCCAA
PUP21	TTTCAGTACCTCAAACGAAGAACTGT	AGTACCACACAAGTTGCAACTAG
VPS53	GCTTGTGGCCCAAGTACATC	GGTAGCCTAGCGTTAAATTTG
VPS53-P	GATGTTGCTGGTTAGCCTCTT	GGGAGAGTAATCTGCTAGGTAG
SULTR4.1	GAAGTACTCCTGCTCTTGG	AGACGCAACATGACACAAC
SULTR4.2	GGCTTCAACCAATATACGG	CGAATAAGCCATCCAAGCC
SRP54	TACTGAGTTGTGATTCTTGC	AATGCTAAATCAATGCCATGA
SRP54-1	GCTGACAGGAAAAATGCTAAT	CTCATCCATATGCTCTCCTGTTC
PHT1.1	CTCTAGGAAATGGCCGAA	CCATTTAGTTGGATCTTAAACC
PHT1.2	GAGAGGCTTAGATGGCTGA	CCATTTAGTTGGATCTTAAACC
PHT1.3	GCGTACGATCTCTTTTGTGT	CATTAGTTGGATCGCAAACC

**Supplementary Table 6. Genotyping primers for T-DNA lines**

Gene	T-DNA Line	Primer name	Primer sequence (5'-3')
PUP7	SALK_084103	LP	TAAAGACACCCTCCATGTTCC
		RP	GAGAACTACACAACCTCGCAAC
		LB	ATTTTGCCGATTTTCGGAAC
PUP8	SALK_137526	LP	TCGTTGTTGACTTCCAAATCC
		RP	TGAGGATCAGTTGTACCAGGG
		LB	ATTTTGCCGATTTTCGGAAC
PUP21	GK-288E11	LP	AGCAAAAGGTACCTGATGACG
		RP	CTTTTCGTTCGAGGTAGTGCTG
		LB	ATAATAACGCTGCGGACATCTACATT

**Supplementary Table 7. PUP cloning**

Cloning primers. Gene	Forward primer (5'-3')	Reverse primer (5'-3')
<i>PUP7</i> genomic	caccATGGACAGATCTCAAGAACACTA TGCC	TCACACACTTTGTATGTTTGTGTGAC C
<i>PUP8</i> CDS	caccATGGAAATAACTCAAGTAATCTA TGT	TCATACACTATGTATGTTTGTGTGAC CTTCC
<i>PUP21</i> CDS	caccATGGGCATATCTCAAGTACACTA TTGC	TCATAAAGTTTGTGTTTCTTCCTCAA CAGGTT

**Supplementary Table 8. MRM transitions for LC-MS/MS analysis.**

Analyte	Retention Time [min]	Q1 [m/z]	Q3 [m/z]	CE [eV]	Reference
tZ [M+H] <sup>+</sup>	1.25	220.0	136.0 <sup>Qt</sup>	15	(Ionescu et al. 2017)
tZR [M+H] <sup>+</sup>	1.40	352.0	220.0 <sup>Qt</sup>	15	(Ionescu et al. 2017)
iPR [M+H] <sup>+</sup>	1.60	336.1	204.0 <sup>Qt</sup>	15	(Ionescu et al. 2017)
		336.1	136.0	27	
		336.1	148.0	23	

Qt = quantifier ion, additional transitions were used for identification only; CE=collision energy; Q=quadrupole.

**References:**

1. Shimada, T. L., Shimada, T. & Hara-Nishimura, I. A rapid and non-destructive screenable marker, FAST, for identifying transformed seeds of *Arabidopsis thaliana*: TECHNICAL ADVANCE. *Plant J.* **61**, 519–528 (2010).